 doi:10.20944/preprints202201.0063.v1

Article

Potent Antiplasmodial Derivatives of the Antitussive Drug Dextromethorphan Reveal the Ent-Morphinan Pharmacophore of Tazopsine-Type Alkaloids

Antoinette Keita,[#] Jean-François Franetich,[¥‡] Maëlle Carraz,[¢‡] Loïse Valentin,[¥Ø‡] Mallaury Bordessoulles,[¥] Ludivine Baron,[¥] Pierre Bigeard,[¥] Florian Dupuy,[Δ∇] Valentine Geay,[‼] Maurel Tefit,[¥] Véronique Sarrasin,[‖] Sylvie Michel,[‼]Catherine Lavazec,[Δ∇] Sandrine Houzé,[#‖] Dominique Mazier,[¥] Valérie Soulard,[¥] François-Hugues Porée[₣*] and Romain Duval[#*]

[#] Université de Paris, UMR 261 - MERIT, IRD, 4 Avenue de l'Observatoire, 75006 Paris, France.
[¥] Sorbonne Université, INSERM, CNRS, Centre d'Immunologie et des Maladies Infectieuses, 75013 Paris, France.
[¢] Université de Toulouse, UMR 152 Pharma-*Dev*, IRD, UPS, Toulouse, France.
[Ø] Biopredic International, Parc d'affaires de la Bretèche, Bldg A4, 35760 Saint-Grégoire, France.
[Δ] Laboratoire d'excellence GR-Ex, Paris, France.
[∇] Université de Paris, Inserm U1016, CNRS UMR 8104, Institut Cochin, Paris, France.
[‼] Université de Paris, UMR 8038 - CNRS CiTCoM, 4 Avenue de l'Observatoire, 75006 Paris, France.
[₣] Université de Rennes 1, ISCR UMR CNRS 6226, Faculté de Pharmacie, 2 Avenue du Pr Léon Bernard, 35000 Rennes, France.
[‖] CNR du Paludisme, AP-HP, Hôpital Bichat-Claude-Bernard, 46 Rue Henri-Huchard, 75018 Paris, France.
‡ These authors contributed equally.
* Correspondence: francois-hugues.poree@univ-rennes1.fr; RD: romain.duval@ird.fr

Abstract: The alkaloid tazopsine **1** was introduced in the late 2000's as a novel antiplasmodial hit compound active against *Plasmodium falciparum* hepatic stages, with potential to develop prophylactic drugs based on this novel chemical scaffold. However, the structural determinants of tazopsine **1** bioactivity, together with the exact definition of the pharmacophore, remained elusive, impeding further development. We found that the antitussive drug dextromethorphan (DXM) **3**, although lacking the complex pattern of stereospecific functionalization of the natural hit, was harboring significant antiplasmodial activity *in vitro* despite suboptimal prophylactic activity in a murine model of malaria, which precluded its direct repurposing against malaria. The targeted *N*-alkylation of *nor*-DXM **15** delivered a small library of analogues with greatly improved activity over DXM **3** against *P. falciparum* asexual stages. Amongst these, *N*-2'-pyrrolylmethyl-*nor*-DXM **16i** showed a 2- to 36-fold superior inhibitory potency compared to tazopsine **1** and DXM **3** against parasite liver and blood stages, with 760 ± 130 nM and 2.1 ± 0.4 µM IC_{50} values, respectively, as well as liver/blood phase selectivity of 2.8. Furthermore, cpd. **16i** showed a 5 to 8-fold increase of activity relatively to DXM **3** against *P. falciparum* stages I-II and V gametocytes, with 18.5 µM and 13.2 µM IC_{50} values, respectively. Cpd. **16i** can thus be considered a promising novel hit compound against malaria in the *ent*-morphinan series with putative pan-cycle activity, paving the way for further therapeutic development (e. g., investigation of its prophylactic activity in a mouse model of malaria).

Keywords: Malaria; *Plasmodium berghei*; *Plasmodium falciparum*; hepatic stages; blood stages; prophylaxis; tazopsine; dextromethorphan; *N*-alkylation; hit compounds

1. Introduction

Malaria remains the major parasitic disease in the world, responsible for 229 million cases in 87 countries in 2019, associated with > 400,000 deaths.[1] Malaria is also the most important infectious cause of mortality in children between 5 and 14 year

Preprints (www.preprints.org) | NOT PEER-REVIEWED | Posted: 6 January 2022 doi:10.20944/preprints202201.0063.v1

old,[2] principally from the deadliest and Africa-prevalent *Plasmodium falciparum* parasite species.[3] Malaria begins with the bite of a *Plasmodium*-infected female *Anopheles* mosquito, which injects sporozoites into the skin of the mammalian host. Sporozoites readily travel into the bloodstream, traverse a few liver cells and finally home into a hepatocyte. Once inside the host cell, sporozoites actively replicate and turn into multinucleated hepatic schizonts. At the end of the hepatic phase (i. e., 2-14 days after initial invasion, depending on the *Plasmodium* species), schizont and host cell rupture, releasing thousands of merozoites into the blood stream. Merozoites invade red blood cells inside which they actively replicate leading to schizonts, releasing merozoites which re-infect other erythrocytes in an exponential fashion. The symptomatology of malaria is directly associated with the parasite developmental phase in the blood, which is the principal target of most antimalarial drugs.[4]

Semisynthetic artemisinin derivatives (ARTDs), associated to longer half-life companion drugs in Artemisinin Combination Therapies (ACT), exert fast curative action against parasite blood stages and remain the frontline antimalarials prescribed worldwide. However, ARTDs are threatened by the rapid spread of artemisinin-resistant *P. falciparum* strains in South-East Asia[5] and their independent emergence recently in Africa,[6-8] which manifest a delayed clearance phenotype under conventional drug regimens.[9] This phenomenon is a worrying continuum of the history of chemoresistance by malaria parasites, which most exclusively affects drugs targeting the parasite blood phase. Indeed, *Plasmodium* erythrocytic phase is characterized by important parasitemia and high mutations rates, allowing the selection of drug-resistant mutants.[4, 10] On the other hand, the initial asymptomatic hepatic phase of parasite development features lower parasitemia and consequently lower mutation events, being thus considered an attractive target for malaria chemoprophylaxis. Drugs possessing novel chemical scaffolds active against parasite hepatic stages, either selectively[11] or as part of a pan-active mode of action,[12-13] are therefore strongly pursued in drug discovery programs.

Tazopsine **1**, a novel *ent*-morphinan alkaloid isolated from the endemic Malagasy plant *Strychnopsis thouarsii* (Figure 1), induces low micromolar inhibition of *P. falciparum* liver and blood stages *in vitro*, but is insufficiently prophylactic at subtoxic dose in mouse infected by *P. yoelii* (70 % protection at 100 mg/kg). On the other hand, the semisynthetic derivative *N*-cyclopentyltazopsine **2** is 10-fold less active but 15-fold more selective than **1** towards liver stages *in vitro*. **2** is also less toxic than **1**, enabling full prophylaxis at 200 mg/kg in the aforementioned malaria mouse model.[14] Despite patents filled in 2004 and 2006, these unprecedented antimalarial hits were not further investigated due to the difficult bio-sourcing of **1**, its complex chemical structures from total synthesis viewpoints, limited structure-activity relationships (SAR)[14-15] as well as absence of identified pharmacophore and molecular targets in the series. Interestingly, antiplasmodial properties are shared by other *ent*-morphinan alkaloids,[15-16] suggesting the existence of a common pharmacophore irrespective of substitution or stereochemical patterns. Based on this rational, we identified the generic antitussive drug dextromethorphan **3** (DXM, *alias* 3-methoxy-17-methylmorphinan) as possibly integrating the essential functional features of these alkaloids (Figure 1), having in mind its direct repurposing against malaria or its use to access simplified mimics of bioactive *ent*-morphinan alkaloids. The present paper describes the results of these endeavors.

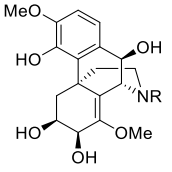

R = H: Tazopsine **1**
R = cyclopentyle: *N*-cyclopentyltazopsine **2**

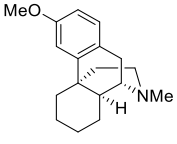

Dextromethorphan **3**
(DXM)

Preprints (www.preprints.org) | NOT PEER-REVIEWED | Posted: 6 January 2022 doi:10.20944/preprints202201.0063.v1

Figure 1. Antiplasmodial *ent*-morphinans: natural tazopsine **1**, semisynthetic hit **2** and the prospected DXM **3**.

2. Results

Extended SAR in the tazopsine series.

We present here pharmacomodulation efforts towards novel derivatives of tazopsine **1**. Altogether, these SARs drove the validation of DXM **3** as a general and simplified mimick of all natural *ent*-morphinan alkaloids, and subsequently guided its chemical diversification into optimized antiplasmodial derivatives. Tazopsine **1** was treated with excess diazomethane to give the 4-methyl phenol ether **6** with 39 % yield. The native alkaloid was in parallel submitted to reductive amination with various aldehydes in presence of sodium cyanoborohydride, to deliver tertiary amines **7a-g** with 45-82 % yields. To assess the influence of a basic nitrogen on the antiplasmodial activity, *N*-acetyl-tazopsine **8** was produced by treating tazopsine **1** with acetic anhydride, with 46 % yield (Figure 2).

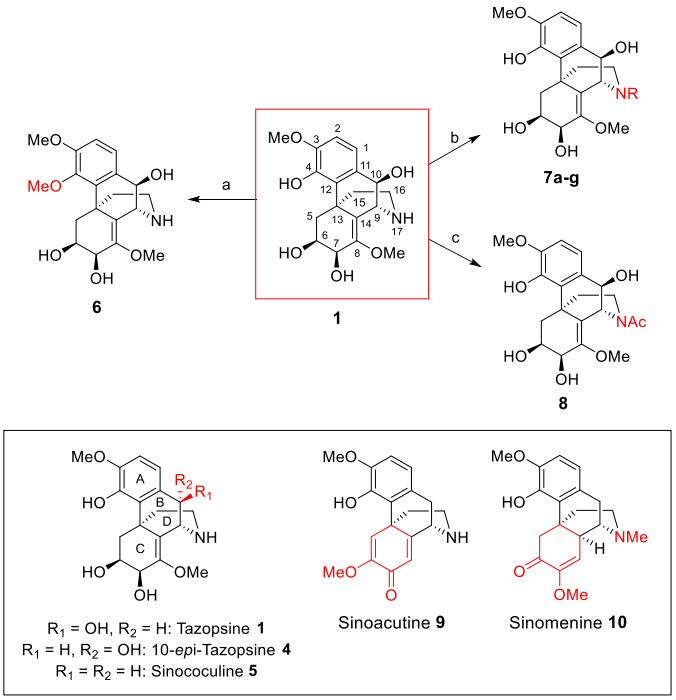

Figure 2. Semisynthetic access to tazopsine derivatives **6**-**8** and structure of natural *ent*-morphinan alkaloids for SAR generation (morphine numbering). (a) CH_2N_2, MeOH, 0 °C, 12 h (39 %); (b) aldehyde (1.1 eq), MeOH, r. t., 10 min then $NaBH_3CN$ (1 eq), r. t. (45-82 %); (c) Ac_2O (1 eq), MeOH, r. t., 1 h (45 %). The box indicates the natural alkaloids.

Primary mouse hepatocytes (PMH) infected by the murine parasite *P. yoelii* were used to assess the bioactivity of the generated tazopsine derivatives (Table 1), allowing direct comparison with previously generated SAR in the series.[14-15] ***Benzylic 10-substitution (ring B) SAR:*** comparison of tazopsine **1**, 10-*epi*-tazopsine **4** and sinococuline **5** to assess the effect of benzylic 10-substitution showed that the 10-(*R*)-hydroxy pattern of tazopsine **1** was optimal, its 10-epimer **4** being 5-fold less active. On the other hand, a completely unsubstituted pattern proved only slightly less beneficial, showed by the comparable bioactivities of tazopsine **1** and sinococuline **5**. ***Aryl 4-O-substitution (ring A) SAR:*** alkylation of tazopsine **1** free phenol abolished the antiplasmodial activity, with 4-*O*-methyl-tazopsine **6** showing unsignificant inhibitory effects against the parasite at 100 µM. ***17-N-substitution (ring D) SAR:*** tertiary amine derivatives of tazopsine **1** showed loss of activity with increase of substituent size (*N*-methyl-tazopsine **7a** already been 2-fold less active than the parent alkaloid) but this trend was mitigated by the beneficial *N*-4′-halo-benzyle substituents in

Preprints (www.preprints.org) | NOT PEER-REVIEWED | Posted: 6 January 2022 doi:10.20944/preprints202201.0063.v1

analogues **7f** and **7g**, exhibiting similar levels of inhibition than tazospine **1**. This suggests that specific substituents can favorably impact on the antiplasmodial activity of *N*-modified *ent*-morphinans in spite of relative bulkiness, a trend already observed for *N*-cyclopentyltazopsine **2** (IC_{50} = 3.5 ± 0.1 μM).[14] On the other hand, *N*-acetyl-tazopsine **8** was completely devoid of activity, suggesting that the presence of a nitrogen atom either basic (i. e., protonated at physiological pH values) or capable of engaging donating hydrogen bonds was important for the antiplasmodial properties. ***Cyclohexenol/enone/dienone (ring C) SAR:*** comparison of tazopsine **1** with sinoacutine **9** and sinomenine **10** revealed that the southern portion of these alkaloids exerted a profound influence on their bioactivity. Indeed, only the 6,7-dihydroxy-8,14-methylenol moiety of tazopsine **1** correlated with strong antiplasmodial effects, while the distinctive methoxy-enone/dienone systems present in **9** and **10** led to abolished activity (Figure 2). In conclusion of these SAR in the *ent*-morphinane series, it appeared that the benzylic substitution at C-10 in ring B had to be either (*R*)-hydroxyl (as in tazopsine **1**) or non-existent (as in sinococuline **5** and DXM **3)**. The ring A in tazopsine **1** seems to be a sensitive part to modify considering the loss of activity of 4-*O*-methyltazopsine **6**, albeit this punctual variation should preclude premature conclusions. *N*-alkylation in the tazopsine series consistently appeared as a relevant pharmacomodulation at ring D with frequent conservation of antiplasmodial activity. Last, SAR regarding the southern ring C of *ent*-morphinans remains unconclusive except for the restricted benefit of that present in tazopsine **1**, a fact corroborated by the previous description of bioactivity loss of the tazopsine-6,7-acetonide.[14]

Table 1. Antiplasmodial activity of tazopsine derivatives **6**-**8** and of natural *ent*-morphinan alkaloids against *P. yoelii* liver stages. NA: non-applicable.

Cpd.	Substitutions	IC_{50} (Py265BY-PMH, μM)
Tazopsine **1**	R_1 = OH, R_2 = H	3.1 ± 0.2
10-*epi*-Tazopsine **4**	R_1 = H, R_2 = OH	16.1 ± 1.9
Sinococuline **5**	R_1 = R_2 = H	4.5 ± 0.4
4-*O*-Me-tazopsine **6**	NA	> 100
N-Methyl-tazopsine **7a**	R = Me	5.8 ± 0.4
N-*n*-Propyl-tazopsine **7b**	R = *n*-Pro	12.6 ± 1.7
N-4'-hydroxybenzyl-tazopsine **7c**	R = 4-OH-Bn	14.2 ± 2.2
N-4'-Methoxybenzyl-tazopsine **7d**	R = 4-OMe-Bn	24.2 ± 0.7
N-3',4'-methylenedioxybenzyl-tazopsine **7e**	R = 3,4-methylenedioxy-Bn	> 100
N-4'-Chlorobenzyl-tazopsine **7f**	R = 4-Cl-Bn	5.8 ± 1.1
N-4'-Bromobenzyl-tazopsine **7g**	R = 4-Br-Bn	4.2 ± 0.3
N-Acetyl-tazopsine **8**	R = Ac	> 100
Sinoacutine **9**	NA	> 100
Sinomenine **10**	NA	> 100
PQ	NA	0.62 ± 0.03

DXM repurposing against malaria.

DXM **3** is a well-known antitussive drug also used as pain reliever, as well as a dissociative anesthetic and hallucinogen in recreational uses.[17-18] Its pharmacology in the central nervous system (CNS) is well established. Despite being considered a synthetic opiate, DXM **3** does not act at the level of opioid receptors, binding instead with high affinity to sigma receptors as an agonist and to a lesser extent to the phencyclidine channel of *N*-methyl-D-aspartate (NMDA) receptors as an antagonist.[18] The relationship between the neuropharmacology and the antitussive effects of DXM **3** is poorly understood.[17] The similarity of DXM **3** with tazopsine **1** in term of *ent*-morphinan backbone prompted us to evaluate its antiplasmodial properties both *in vitro* and *in vivo*, having in mind its possible direct repurposing against malaria. In a preliminary screen against primary human hepatocytes (PHH) infected by *P. falciparum in vitro*, DXM **3** exhibited an activity that was only 2-fold less than that of tazopsine **1** (Table 2). Noteworthily, the IC_{50} value of tazopsine **1** was slightly above

Preprints (www.preprints.org) | NOT PEER-REVIEWED | Posted: 6 January 2022 doi:10.20944/preprints202201.0063.v1

that previously described of *ca*. 4 µM in this biological model.[14] This observation can be explained by the shift in the PHH used for *P. falciparum* culture from clinical samples in the previous study to standardized, commercially available cryopreserved PHH in the present work. The whole assay was validated by the expected submicromolar activity of the reference drug primaquine (PQ).[14]

Table 2. *In vitro* IC_{50} values of tazopsine **1** and DXM **3** against *P. falciparum* liver stages. IC_{50} values are the mean of four technical replicates.

Cpds.	IC_{50} (PHH, µM)
Tazopsine **1**	7.88 ± 3.05
DXM **3**	15.59 ± 1.19
PQ	0.75 ± 0.15

Following the exciting discovery of the antiplasmodial activity of DXM 3 against *P. falciparum* liver stages *in vitro*, we tested its prophylactic potential in a *P. berghei*-infected mouse model of malaria. We used the transgenic parasite line *P. berghei*-Luc infecting BALB/c mice to follow parasitemia *in situ* based on the spontaneously emitted bioluminescence after injection of D-luciferine.[19] Following a preliminary study, we found that DXM 3 induced convulsive episodes and death in mouse at doses superior to 60 mg/kg administered daily (data not shown). Therefore, we decided to use a subtoxic regimen of 40 mg/kg DXM 3 administered daily starting 24 h before infection and further maintained for a 48 h period, corresponding to the duration of *P. berghei* liver phase. In addition, we chose to associate DXM 3 with quinidine (QND), a known inhibitor of CYP2D6-mediated *O*-demethylation of DXM 3 into its main hepatic metabolite dextrorphan 12 (DX, *syn.* 3-hydroxy-17-methylmorphinan),[18] as a way to increase the plasmatic half-life of DXM 3[20-21] and possibly increase its antimalarial effect *in vivo*. DXM 3 at 40 mg/kg and QND at 20 mg/kg were deprived of prophylactic activity in this *in vivo* model, with parasitemia levels not significatively different between these groups and the vehicle (Figure 3). While the combination of DXM 3 and QND at a daily regimen of 40 mg/kg and 20 mg/kg, respectively, exerted significative prophylactic inhibition of *P. berghei*-Luc growth, we found that this synergistic combination was far from eliciting complete parasite clearance as did the reference drug primaquine biphosphate at a daily regimen of 5 mg/kg (Figure 3).

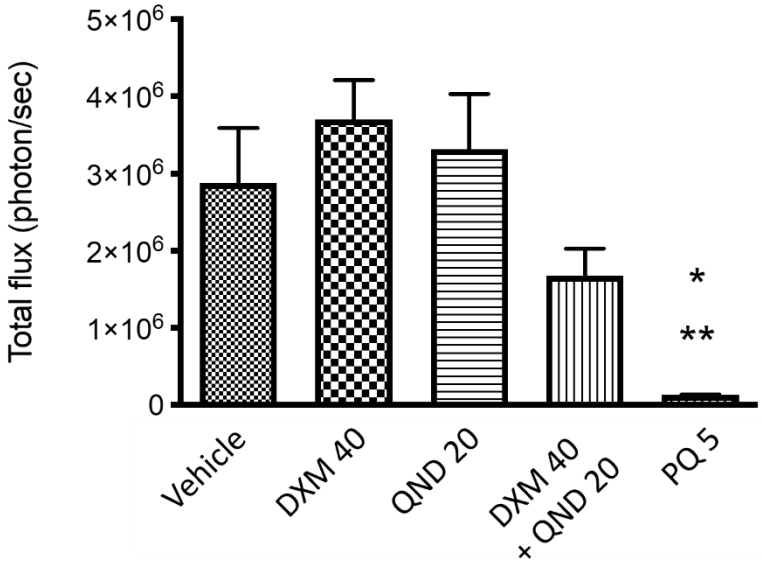

Figure 3. *In vivo* prophylactic activity of DXM **3** +/- QND compared to PQ in a mouse model of *P. berghei*-Luc infection. Each group of mice consisted of five individuals. Results are shown as mean +/- SEM. * Vehicle *vs* PQ: $p = 0.0124$; ** DXM40 *vs* PQ and QND20 *vs* PQ: $p < 0.05$ (Anova one-way test for multiple comparisons). Numeric values indicate doses in mg/kg.

Preprints (www.preprints.org) | NOT PEER-REVIEWED | Posted: 6 January 2022 doi:10.20944/preprints202201.0063.v1

The extend of DXM **3** metabolization *in vivo* into DX **12** (theoretically inhibited by QN) and to a lesser part into *nor*-DXM **15** (*syn.* 3-hydroxy-17-methylmorphinan) by CYP3A4-mediated *N*-demethylation[18, 22] remains uncharacterized in our study. If effective and yielding inactive metabolites, its occurrence could explain the relatively poor prophylactic activity of DXM **3** in this mouse model of malaria. However, this outcome proved to be invalid as both DX **12** and *nor*-DXM **15** were later synthesized (Figure 4) and found to have similar level of inhibitory potency *in vitro* than DXM **3** against *P. berghei* (Figures 5 & 6). Despite the unlikeliness of its repurposing as a prophylactic drug against malaria, DXM **3** represents a readily accessible and flexible synthetic platform to explore the antimalarial potential of the *ent*-morphinan series and circumvents the inherent limitations of the tazopsines.

DXM pharmacomodulation towards improved antiplasmodial derivatives.

DXM **3**, possessing the same backbone as the natural hit tazopsine **1**, constituted the synthetic starting point of our study. This compound combines two advantages for a SAR study: *(i)* straightforward and cheap access from various commercial suppliers in gram quantities, and *(ii)* easy functionalization on the C-2 and/or *O*- and/or *N*-positions (Figure 4). To explore yet unraveled SAR on the aryl ring, DXM **3** was firstly *o*-iodinated using NIS to deliver 2-I-DXM **11** with a 91 % yield. DX **12** was obtained as described by Jakobsson *et al.*[23] by the *O*-demethylation of DXM **3** with 48 % aqueous HBr, then *o*-iodinated with NIS in the previous conditions to yield 2-I-DX **13** with a 87 % yield (Figure 4). As previously observed with tazopsine **1**, derivatization of the nitrogen position revealed to be a relevant modification with retainment of the antiplasmodial activity (Table 1) and possible improvement of the antimalarial profile.[14] Therefore, *N*-modification of *nor*-DXM **15** was decided to be fully explored. Towards this aim, DXM **3** free base was *N*-demethylated *via* the trichloroethylcarbamate intermediate **14** as described by Jozwiak *et al.*[24] to give *nor*-DXM **15**. Reductive amination, particularly using sodium triacetoxyborohydride (STABH) as reductant, represents a mild and chemoselective method for the *N*-alkylation of primary and secondary amines.[25] Tertiary amines **16a**-**m** were thus synthesized from *nor*-DXM **15** using *n*-alkyl, cycloalkyle, heteroaryle and *bis*-heteroaryle aldehydes in presence of STABH with moderate to good yields (33-99%) (Figure 4). To decipher the influence of the protonation state of the nitrogen atom on the antiplasmodial activity of *ent*-morphinans - taking into account that tazopsine **1**, *N*-cyclopentyltazopsine **2**, DXM **3**, DX **12**, *nor*-DXM **15** and its *N*-alkyle derivatives **16a-m** are to be fully protonated at physiological pH values - two compounds **17** and **18** with a neutral or constitutively positive charge on the nitrogen atom, respectively, were synthesized. Cpd. **17**, corresponding to the exact amide congener of the amine **16d** for the sake of precise SAR comparison, was prepared by reacting *nor*-DXM **15** with cyclopropanecarbonyle chloride in presence of triethylamine, with excellent yield. On the other hand, the quaternary ammonium **18** was obtained in high yield by reacting DXM **3** free base with methyl iodide (Figure 4).

Preprints (www.preprints.org) | NOT PEER-REVIEWED | Posted: 6 January 2022 doi:10.20944/preprints202201.0063.v1

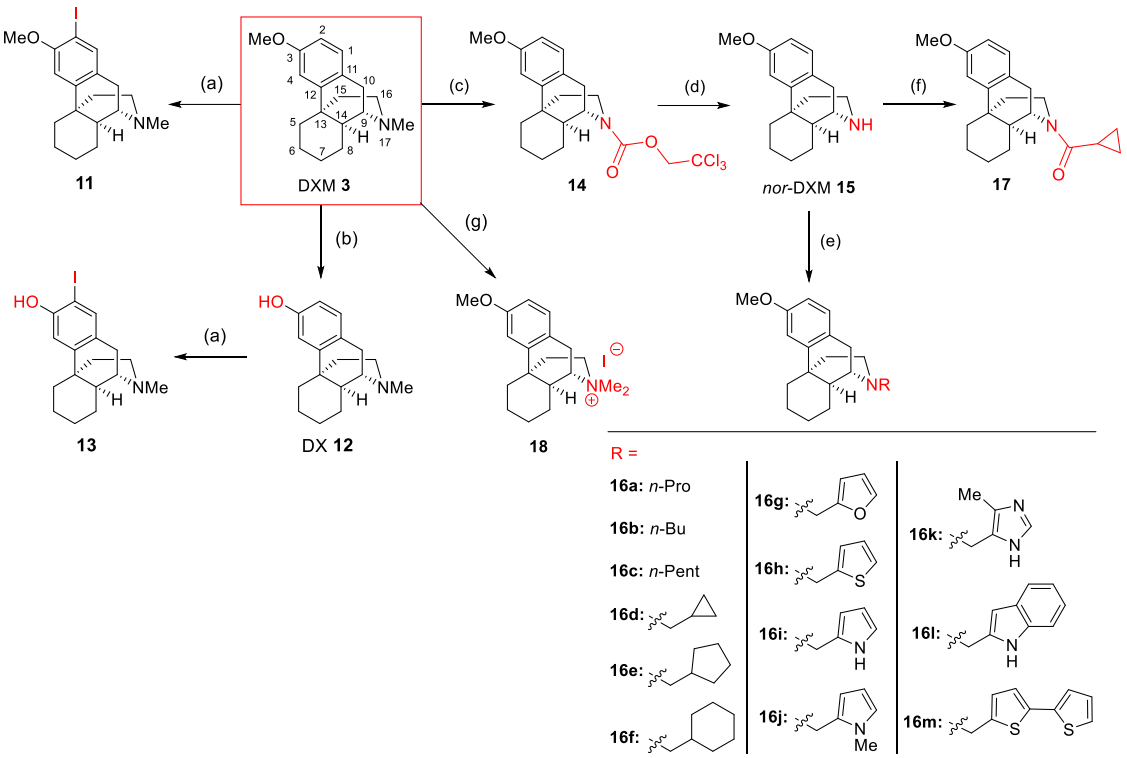

Figure 4. Semisynthetic access to DXM derivatives **11-18** for SAR generation (morphine numbering). (a) NIS (1.15 eq), *p*-TsOH (1.8 eq) (91 % **11**, 87 % **13**); (b) HBr 48%, reflux overnight (91 %) (c) 2,2,2-trichloroethylchloroformate (1.1 eq), toluene, reflux, 2 h (92 %); (d) Zn powder (3 eq), AcOH, r. t., 1 h (47 %); (e) aldehyde (1.1 eq), DMF, r. t., 10 min then STABH (2 eq), r. t. (33-97 %); (f) cyclopropanecarbonyle chloride (1.1 eq), CH_2Cl_2, Et_3N, 0°C to r. t, 1.5 h (75 %); (g) MeI, rt, 2 h (82 %).

In vitro pre-screening against P. berghei liver stages.

The antimalarial activity against liver stages of the obtained 21-compound library was first pre-screened using PHH infected by *P. berghei* expressing the Green Fluorescent Protein (PHH-*Pb*-GFP). This model has the advantage of being less expensive and more accessible than the hepatic stages of *P. falciparum*, thanks to routine production of *P. berghei* sporozoites in the laboratory, while using the same host cell than for the human parasite and therefore being representative of parasite-host cell interactions. Compound activity was assessed by two criteria, *(i)* the number of parasites developing within PHH (Exo-Erythrocytic Forms, EEFs, Figure 5A) and *(ii)* the size of parasites (μm^2) normalized on untreated controls (Figure 5B). False positives, due to compound toxicity against host PHH, were excluded by normalizing parasite number on nuclei number of untreated controls. At the highest concentration (20 µM), viability of PHH was > 80 % for the less active compounds and 50-60 % for the most active ones. Four activity profiles could be categorized from the 21-compound library screening in terms of EEFs number (Figure 5A), namely: *(i)* inactive compounds (2-I-DX **13**, **14**, **16f**, **16h**, **16j**, **17**, **18**); *(ii)* low-activity compounds with similar inhibitory potency than DXM **3** (DX **12**, *Nor*-DXM **15**, **16b**, **16c**, **16d**, **16e**, **16k** and **16m**); *(iii)* active compounds (2-I-DXM **11**, **16a**, **16g**, and **16l**); (*iv*) one very active compound (**16i**). These activity ranges were respectively characterized by *(i)* a high EEFs number at 20 µM (the maximal concentration of the range), *(ii)* a low EEFs number at 20 µM, *(iii)* a low EEFs number at 10 µM and finally *(iv)* a low EEFs number at 1 µM. We observed the same trend in the plot of parasite size (Figure 5B) with a delineation for cpd. **16i** exhibiting an important size effect at 1 µM, followed by cpds. **11**, **16c**, **16e**, **16g**, and **16l** at 10 µM. In the light of these results, we focused on molecules possessing an inhibitory activity between 1-10 µM and established an amplified cut-off test at the arbitrary concentration of 7 µM to validate the above-described categories

 doi:10.20944/preprints202201.0063.v1

of inhibitors (Figure 6). This evaluation permitted to identify which compounds inhibited liver stage parasite development (e. g. leading to a 50 % reduction in EEFs number normalized on the drug-free controls. Five molecules were thus validated in the cut-off test, i. e. cpds. **16c**, **16d**, **16i**, **16l** and **17** (Figure 6A). In addition, **16e** was halfway and susceptible to have interesting activity. A low EEFs size effect was observed for cpds. **16g**, **16h**, **16i**, **16l** and **16m** but none of these molecules inhibited parasite size by at least 50 % (Figure 6B). Regarding substitution of DXM **3** or DX **12** with iodine on the C-2 position, only 2-I-DXM **11** exhibited a gain

 doi:10.20944/preprints202201.0063.v1

of potency relatively to the parent compound while 2-I-DX 13 was inactive (Figure 5). Interestingly, amine **16d** and its amide congener **17** displayed similar levels of inhibitory activity against *P. berghei* liver stages (Figures 5 and 6). This suggested that the presence of an electro-donating doublet on the nitrogen atom rather than that of a protonated one was an important feature for the interaction of *ent*-morphinans with their biochemical target(s). However, this behavior was contradictory with that observed in the tazopsine series where *N*-acetylation abolished the activity (Table 1). Nevertheless, this trend in the DXM series was reinforced by a lower activity of the quaternary ammonium **18** compared to DXM **3** (Figure 5). This showed that in spite of the intrinsically charged state of most bioactive DXM derivatives at physiological pH (with exception of cpd. **17**), the presence of a permanently charged nitrogen atom was detrimental to the antiplasmodial activity.

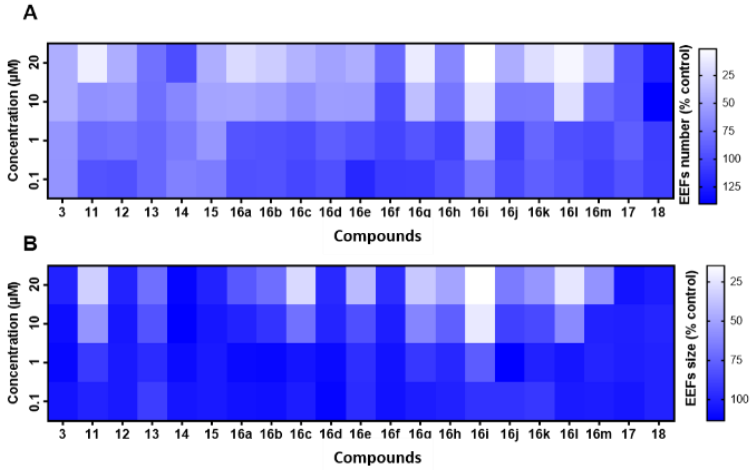

Figure 5. Normalized dose-response heatmap in PHH-*Pb*-GFP regarding EEFs number (**A**) and EEFs size (**B**) at 0.1, 1, 10 or 20 µM of the indicated compounds. These results were obtained from four technical replicates.

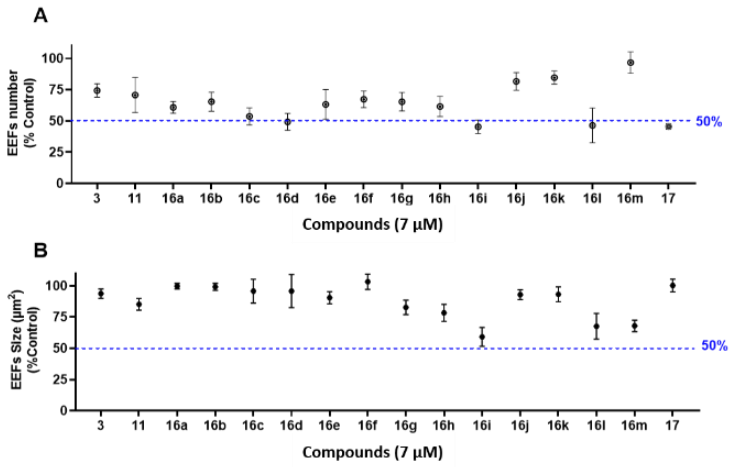

Figure 6. Normalized EEFs number (**A**) and EEFs size (**B**) in PHH-*Pb*-GFP at the arbitrary cut-off value of 7 µM for the indicated compounds. Each point (•) represents the average of EEFs number of four technical replicates. The error bars represent the interval of variability between EEFs number. These results were obtained from four technical replicates.

In vitro screening against P. falciparum liver and asexual blood stages.

2-I-DXM **11**, **16a** (R = *N*-propyl), **16g** (R = *N*-2-furanylmethyl), **16i** (R = *N*-2′-pyrrolylmethyl) and **16l** (R = *N*-2′-indolylmethyl), which displayed the best inhibitory effects in

Preprints (www.preprints.org) | NOT PEER-REVIEWED | Posted: 6 January 2022 doi:10.20944/preprints202201.0063.v1

the *P. berghei* pre-screening, were selected for screening against both liver and blood stages of the human parasite *P. falciparum* and determination of their IC_{50} values. PQ and chloroquine (CQ) were used as reference drugs against liver and blood stages, respectively. Compound toxicity against host PHH was excluded by normalizing parasite number on nuclei number of untreated controls. At 10 μM, viability of PHH was *ca.* 100 % for the less active compounds and 60-70 % for the most active ones. The observed gain of antiplasmodial activity of 2-I-DXM **11** compared to DXM **3** against *P. berghei* liver stages was confirmed against *P. falciparum*, the latter being 4-fold more active than the parent compound (Table 3). Regarding the pre-screened *N*-modified analogues **16a**, **16g**, **16i** and **16l**, these were active against *P. falciparum* liver stages in the low micromolar/submicromolar range and displayed significantly lower IC_{50} values than both parent compounds, i. e. the natural hit tazopsine **1** and DXM **3** (Tables 1 and 3). The most active compound was the *N*-2'-pyrrolylmethyl derivative **16i** which strongly inhibited the development of parasite liver stages, being 10-fold more active than tazopsine **1** (Table 1) and 20-fold more active than DXM **3** (Table 3). Strikingly, cpd. **16i** showed a superimposable inhibitory potency to the antimalarial drug PQ against *P. falciparum* liver stages (IC_{50} values of 0.76 ± 0.13 μM and 0.75 ± 0.15 μM, respectively). Cpd. **16i** was also very active on the parasite blood stages (IC_{50} values of 2.1 ± 0.4 μM), again similarly to PQ with reported *ca.* 1-20 μM IC_{50} values against the *P. falciparum* 3D7 strain.[26-27] Besides **16i**, only **16l** showed activity in the low micromolar range against *P. falciparum* blood stages (IC_{50} of 6.5 ± 0.4 μM). Other *N*-alkylated derivatives exhibited low activity against blood stages, similarly to DXM **3** with IC_{50} values of 43-62 μM. However, all compounds were found to be selective for the hepatic phase of parasite development (2.8-36-fold selectivity) including DXM **3** (4.9-fold selectivity) (Table 3).

Table 3. *In vitro* IC_{50} values of tazopsine **1**, DXM **3** and selected *N*-modified derivatives against *P. falciparum* liver (NF54) and blood (3D7) stages, as well as liver phase selectivity values (S). These results were obtained by four technical replicates for PHH and three technical for HE. HE: human erythrocytes; NT = not tested; NA = non-applicable.

Cpds.	IC_{50} (μM)		S
	PfNF54-PHH	Pf3D7-HE	
Tazopsine 1	7.88 ± 3.05	4.07 ± 0.87	0.5
DXM **3**	15.59 ± 1.19	76.5 ± 0.9	4.9
11	4.10 ± 2.77	61.7 ± 5.3	15.0
16a	2.25 ± 3.03	43.3 ± 2.3	19.2
16g	1.56 ± 0.59	56.2 ± 2.7	36.0
16i	0.76 ± 0.13	2.1 ± 0.4	2.8
16l	1.98 ± 0.34	6.5 ± 0.4	3.3
PQ	0.75 ± 0.15	NT	NA
CQ	NT	0.033 ± 0.016	NA

In vitro screening against P. falciparum sexual blood stages.

To explore the activity profile of the new lead cpd. **16i** against other developmental stages of *P. falciparum* , we tested it against early (stage I-II) and late (stage V) gametocytes, the last being responsible for transmission of *P. falciparum* malaria. Cpd. **16i** was found to be fairly effective against both sexual stages with activities in the high micromolar range, whereas DXM **3** was completely inactive (IC_{50} > 100 μM) (Figure 7).

Preprints (www.preprints.org) | NOT PEER-REVIEWED | Posted: 6 January 2022 doi:10.20944/preprints202201.0063.v1

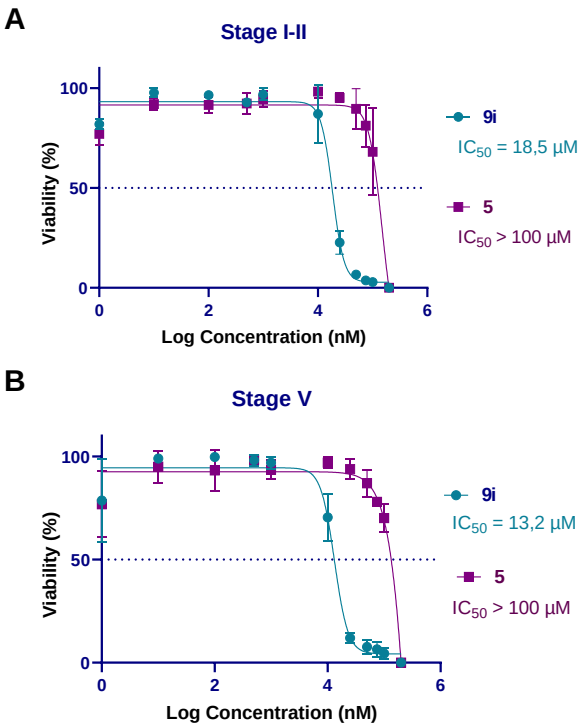

Figure 7. Inhibitory plots and IC_{50} values of DXM **3** (purple) and cpd. **16i** (blue) against *P. falciparum* early (stages I-II) and late (stage V) gametocytes *in vitro*. These results represent the mean of three technical replicates and three biological replicates. Error bars represent standard deviation.

3. Conclusions

This section is not mandatory but can be added to the manuscript if the discussion is unusually long or complex.

Despite the intensive search for novel antimalarial drugs, malaria remains a major disease in tropical regions. The rapid spread of artemisinin resistant *P. falciparum* strains in South-East Asia[5] and independent increase of k13 polymorphisms in Africa,[28-29] which culminated in clinical artemisinin-resistance recently detected in the continent,[6-8] is a dramatic continuum of the drug resistance history of malarial parasites. This situation underscores the need for alternative chemotherapeutic strategies beyond pursuing novel drugs to eliminate blood parasites, prone to readily acquire resistance mutations. In this context, the novel antimalarial alkaloid tazopsine **1**, introduced in the late 2000's, is active against both pre-erythrocytic and erythrocytic *P. falciparum* stages and the precursor of the *in vivo* prophylactic compound *N*-cyclopentyltazopsine **2**. However, development of the tazopsines by bio-sourcing or synthetic strategies appeared difficult. Aiming to overtake these limitations, we managed to simplify the natural alkaloids tazopsine **1** - the same principle applying to the related sinococuline **5** - and to extract a "naked" *ent*-morphinan antiplasmodial pharmacophore under the form of the antitussive drug DXM **3**. In particular, substitutions at the level of rings B and C proved non-essential while those affecting ring A (particularly at C-2) of potential relevance. In spite of limited potential for a repurposing against malaria, DXM **3** exhibited a significant level of bioactivity *in vitro* that was only 2-fold lower than that of tazopsine **1** against *P. falciparum* liver stages. Capitalizing on strengthened ring D SARs, a rapid diversification of DXM **3** into *N*-modified derivatives readily led to improved analogues. Amongst those, the hit cpd. *N*-2′-pyrrolylmethyl-*nor*-DXM **16i** exhibited a 10-fold and 20-fold increase of activity against *P. falciparum* liver stages relatively to tazopsine **1** and DXM **3**, showing similar activity than the reference drug primaquine against parasite liver and blood stages. In the context of prophylactic antimalarial drug discovery, cpd. **16i** was more selective for the parasite liver phase than tazopsine **1** (S = 2.8 *vs* 0.5) in addition to a stronger bioactivity than the natural alkaloid.

Preprints (www.preprints.org) | NOT PEER-REVIEWED | Posted: 6 January 2022 doi:10.20944/preprints202201.0063.v1

Moreover, cpd. **16i** showed a significant effect on the viability of stage I-II and V *P. falciparum* gametocytes compared to the completely inactive DXM **3**. These results warrant further mechanistic investigation of the new hit cpd. **16i** regarding causal prophylaxis (i. e., early sterilization of sporozoites) and possibly pan-activity against multiple parasite stages. In addition, the benefit of C-2 substitution suggests an entry to optimized derivatives in the hit series by means of ring A modifications.

Reagents, solvents and equipment.

Reagents and anhydrous solvents were purchased from Merck-Sigma and were of the highest grade available. DXM **3** hydrobromide monohydrate, sinoacutine **9,** sinomenine **10,** primaquine biphosphate (PQ), chloroquine biphosphate (CQ) and D-luciferin were purchased from Merck-Sigma. Tazopsine **1**, 10-*epi*-tazopsine **4** and sinococuline **5** were isolated from the plant *Strychnopsis thouarsii* as described previously.[14-15] DX **12** and *Nor*-DXM **15** were synthesized according to literature procedures.[23-24] Column chromatography was performed using silica gel 60 (9385 Merck). Thin layer chromatography (TLC) was performed on aluminum plates coated with silica gel 60F254 (554 Merck), visualized with UV light (254 and 366 nm) and revealed with sulfuric vanillin or phosphomolybdic acid reagents. NMR spectra (^{1}H and ^{13}C) were recorded on an Advance Bruker 400 MHz spectrometer or an Oxford Instruments 600 MHz spectrometer equipped with a BBI 600 MHz probe, using solvent signal as an internal standard ($CDCl_3$: δ (^{1}H) 7.26 and δ (^{13}C) 77.16 ppm, d6-DMSO: δ (^{1}H) 2.50 and δ (^{13}C) 39.50 ppm). The *J* coupling constants are given in Hertz (Hz). High-resolution mass spectra (HRMS) were recorded in the ESI mode on a LCT Mass Spectrometer (Waters) equipped with a TOF analyzer.

Synthetic chemistry.

Chemical derivations of tazopsine 1 (4,6,7,10- tetrahydroxy- 8,14- didehydro-3,8-dimethoxymorphinan)

4-*O*-Methyl-tazopsine 6, $C_{19}H_{25}NO_6$. A stirred solution of tazopsine **1** free base (20 mg, 0.057 mmol) in anhydrous MeOH (300 mL) was treated with excess diazomethane at 0 °C for 12 h. After removal of the solvent under reduced pressure, the residue was purified by silica gel column chromatography eluted with CH_2Cl_2/MeOH 0-10 v/v containing 20 % aqueous NH_3, yielding **6** (8 mg, 39 %) as a white solid. ^{1}H NMR (MeOD, 400 MHz): δ 6.81 (d, 1H, 8.4); 6.80 (d, 1H, *J* = 8.4); 4.45 (d, 1H, *J* = 2.1); 4.29 (d, 1H, *J* = 2.1); 4.27 (d, 1H, *J* = 2.6); 3.84 (m, 1H); 3.62 (s, 3H); 3.38 (s, 3H); 3.28 (s, 3H); 2.73 (dd, 1H, *J* = 3.2, 13.2); 2.62 (dd, 1H, *J* = 4.6, 13.9); 2.36 (ddd, 1H, *J* = 3.6, 13.9, 12.4); 2.08 (dd, 1H, *J* = 13.2, 13.2); 1.83 (dd, 1H, *J* = 3.6, 12.3); 1.79 (ddd, 1H, *J* = 4.6, 12.3, 12.4). HRMS (ESI): *m/z* calculated for $C_{19}H_{26}NO_6^+$ [M+H$^+$] = 364.1760. Found = 364.1752.

General procedure for the reductive animation of tazopsine 1 (cpds. 7a-g). *N*-alkyl-tazopsine derivatives were obtained from tazopsine using classical reductive amination of 37 % aqueous formaldehyde or pure aldehydes by $NaBH_3CN$.[30] Briefly, a stirred solution of tazopsine **1** free base (34 mg, 0.097 mmol) in anhydrous MeOH (600 µL) was primed by a gentle stream of argon for 15 s. To this solution were added the aldehyde (0.107 mmol) at r. t. followed after 10 min by $NaBH_3CN$ (95 %, 6.4 mg, 97 µmol). The mixture was stirred at r. t. under argon for 24 h. After removal of the solvent under reduced pressure, the residue was acidified with 1 M HCl, then basified with aqueous NH_3, and dried under vacuum. The residue was purified by silica gel column chromatography eluted with CH_2Cl_2/MeOH (0-10 *v/v* containing 20 % aqueous NH_3).

***N*-Methyl-tazopsine 7a, $C_{19}H_{25}NO_6$,** 82 % yield. ^{1}H NMR (MeOD, 400 MHz): δ 6.90 (d, 1H, *J* = 8.4); 6.83 (d, 1H, *J* = 8.4); 4.70 (d, 1H, *J* = 2.2); 4.30 (dd, 1H, *J* = 1.3, 3.4); 4.21 (d, 1H, *J* = 2.2); 3.88 (m, 1H); 3.87 (s, 3H); 3.70 (s, 3H); 2.98 (ddd, 1H, *J* = 1.3, 4.1, 13.8); 2.51 (dd, 1H, *J* = 3.3, 12.4); 2.47 (s, 3H); 2.26 (m, 2H); 2.18 (dd, 1H, *J* = 13.8, 13.8); 1.95 (m, 2H). HRMS (ESI): *m/z* calculated for $C_{19}H_{26}NO_6^+$ [M+H$^+$] = 364.1760. Found = 364.1764.

***N*-*n*-Propyl-tazopsine 7b, $C_{21}H_{29}NO_6$,** 68 % yield. ^{1}H NMR (MeOD, 400 MHz): δ 6.99 (d, 1H, *J* = 8.4); 6.96 (d, 1H, *J* = 8.4); 4.87 (d, 1H, *J* = 1.9); 4.38 (d, 1H, *J* = 2.97); 3.92 (m, 2H); 3.88 (s, 3H); 3.78 (s, 3H); 3.09 (m, 4H); 2.27 (d, 1H, *J* = 13.4); 2.14 (dd, 1H, *J* = 4.0, 12.3); 1.79 (m, 4H);

Preprints (www.preprints.org) | NOT PEER-REVIEWED | Posted: 6 January 2022 doi:10.20944/preprints202201.0063.v1

1.04 (t, 3H, *J* = 7.3). HRMS (ESI): *m*/*z* calculated for $C_{21}H_{30}NO_6^+$ [M+H$^+$] = 392.2073. Found = 392.2064.

***N*-4′-hydroxybenzyl-tazopsine 7c, $C_{25}H_{29}NO_7$**, 45% yield. ^{1}H NMR (MeOD, 400 MHz): δ 7.35 (d, 2H, *J* = 8.6); 6.99 (d, 1H, *J* = 8.4); 6.92 (d, 1H, *J* = 8.4); 6.85 (d, 2H, *J* = 8.6); 4.41 (d, 1H, *J* = 3.3); 4.2 (m, 2H); 3.98 (ddd, 1H, *J* = 3.5, 3.5, 12.98); 3.88 (s, 3H); 3.78 (m, 4H); 3.05 (m, 3H); 2.73 (ddd, 1H, *J* = 4.1, 13.0, 13.0); 2.23 (m, 3H); 2.08 (dd, 1H, *J* = 2.3, 13.7). HRMS (ESI): *m*/*z* calculated for $C_{25}H_{30}NO_7^+$ [M+H$^+$] = 456.2022. Found = 456.2018.

***N*-4′-methoxybenzyl-tazopsine 7d, $C_{26}H_{31}NO_7$,** 52 % yield. ^{1}H NMR (MeOD, 400 MHz): δ 7.47 (d, 2H, *J* = 8.6); 7.0 (d, 2H, *J* = 8.6); 6.98 (d, 1H, *J* = 8.4); 6.93 (d, 1H, *J* = 8.4); 4.88 (d, 1H, *J* = 2.3); 4.71 (d, 1H, *J* = 2.3); 4.40 (d, 1H, *J* = 2.8); 4.25 (s, 2H); 3.99 (m, 1H); 3.88 (s, 3H); 3.83 (s, 3H); 3.77 (s, 3H); 3.06 (m, 2H); 2.75 (dd, 1H, *J* = 2.8, 12.5); 2.28 (ddd, 1H, *J* = 3.2, 13.6, 13.6); 2.20 (dd, 1H, *J* = 3.9, 13.2); 2.07 (dd, 1H, *J* = 2.1, 13.2). HRMS (ESI): *m*/*z* calculated for $C_{26}H_{32}NO_7^+$ [M+H$^+$] = 470.2179. Found = 470.2170

***N*-3′,4′-methylenedioxybenzyl-tazopsine 7e, $C_{26}H_{29}NO_8$**, 52% yield. ^{1}H NMR (MeOD, 400 MHz): δ 7.91 (s, 1H); 7.76 (d, 1H, *J* = 8.1); 7.54 (d, 1H, *J* = 8.1); 6.93 (d, 1H, *J* = 8.4); 6.88 (d, 1H, *J* = 8.4); 5.92 (s, 2H); 4.78 (s, 2H); 4.77 (d, 1H, *J* = 2.3); 4.56 (d, 1H, *J* = 2.3); 4.33 (d, 1H, *J* = 2.8); 3.91 (m, 1H); 3.82 (s, 3H); 3.75 (s, 3H); 2.98 (dd, 1H, *J* = 3.5, 13.4); 2.65 (dd, 1H, *J* = 4.8, 14.5); 2.45 (m, 1H); 2.2 (dd, 1H, *J* = 13.4, 13.4); 2.15 (dd, 1H, *J* = 3.5, 12.5); 1.98 (ddd, 1H, *J* = 4.8, 12.5, 12.5). HRMS (ESI): *m*/*z* calculated for $C_{26}H_{30}NO_8^+$ [M+H$^+$] = 484.1971. Found = 484.1959

***N*-4′-Chlorobenzyl-tazopsine 7f, $C_{25}H_{28}NO_6Cl$**, 71% yield. ^{1}H NMR (MeOD, 400 MHz): δ 7.48 (d, 2H, *J* = 8.3); 7.32 (d, 2H, *J* = 8.3); 6.89 (d, 1H, *J* = 8.4); 6.82 (d, 1H, *J* = 6.4); 4.69 (s, 2H); 4.65 (d, 1H, *J* = 2.1); 4.55 (d, 1H, *J* = 2.7); 4.43 (d, 1H, *J* = 2.1); 3.89 (m, 1H); 3.84 (s, 3H); 3.61 (s, 3H); 2.96 (dd, 1H, *J* = 3.2, 13.8); 2.61 (dd, 1H, *J* = 4.6, 13.9); 2.39 (ddd, 1H, *J* = 3.7, 12.7, 13.9); 2.15 (dd, 1H, *J* = 13.4, 13.8); 2.02 (dd, 1H, *J* = 3.7, 12.7); 1.94 (ddd, 1H, *J* = 4.6, 12.7, 12.7). HRMS (ESI): *m*/*z* calculated for $C_{25}H_{29}NO_6Cl^+$ [M+H$^+$] = 474.1683. Found = 474.1678.

***N*-4′-Bromobenzyl-tazopsine 7g, $C_{25}H_{28}NO_6Br$**, 61% yield. ^{1}H NMR (MeOD, 400 MHz): δ 7.51 (d, 2H, *J* = 8.4); 7.35 (d, 2H, *J* = 8.4); 6.92 (d, 1H, *J* = 8.4); 6.88 (d, 1H, *J* = 8.4); 4.78 (d, 1H, *J* = 2.2); 4.74 (s, 2H); 4.73 (d, 1H, *J* = 2.2); 4.32 (d, 1H, *J* = 2.7); 3.93 (ddd, 1H, *J* = 2.7, 3.7, 13.3); 3.88 (s, 3H); 3.68 (s, 3H); 3.0 (dd, 1H, *J* = 2.9, 13.9); 2.66 (m, 1H); 2.46 (ddd, 1H, *J* = 3.9, 12.1, 12.1); 2.21 (dd, 1H, *J* = 13.5, 13.5); 2.05 (ddd, 1H, *J* = 4.6, 12.6, 12.6); 1.96 (dd, 1H, *J* = 3.8, 12.6). HRMS (ESI): *m*/*z* calculated for $C_{25}H_{29}NO_6Br^+$ [M+H$^+$] = 518.1178. Found = 518.1166.

***N*-Acetyl-tazopsine 8, $C_{20}H_{25}NO_7$.** To a stirred solution of tazopsine **1** free base (34 mg, 0.097 mmol) in anhydrous MeOH (600 µL) at r. t. was added Ac_2O (0.097 mmol, 9.2 µL). The mixture was stirred at r. t. under argon for 1 h. After removal of the solvent under reduced pressure, the residue was purified by silica gel column chromatography eluted with CH_2Cl_2/MeOH (0-5 *v*/*v*), yielding **8** (17 mg, 45 %) as a white solid. ^{1}H NMR (MeOD, 400 MHz): *first* rotamer: δ 6.88 (d, 1H, *J* = 8.5); 6.81 (d, 1H, *J* = 8.5); 5.85 (d, 1H, *J* = 2.8); 4.39 (d, 1H, *J* = 2.8); 4.26 (dd, 1H, *J* = 1.1, 2.6); 3.68 (dd, 1H, *J* = 5.8, 12.9); 3.85 (s, 3H); 3.81 (m, 1H); 3.62 (s, 3H); 3.03 (ddd, 1H, *J* = 1.1, 4.0, 10.8); 2.78 (ddd, 1H, *J* = 4.7, 12.9, 12.7); 2.23 (dd, 1H, *J* = 5.5, 10.8); 2.15 (dd, 1H, *J* = 4.7, 12.7); 2.0 (s, 3H); 1.94 (ddd, 1H, *J* = 5.8, 12.7, 12.7); *second rotamer*: δ 6.92 (d, 1H, *J* = 8.4); 6.83 (d, 1H, *J* = 8.4); 5.28 (d, 1H, *J* = 2.5); 4.49 (d, 1H, *J* = 2.5); 4.31 (dd, 1H, *J* = 1.1, 2.7); 4.12 (dd, 1H, *J* = 5.7, 13.9); 3.84 (s, 3H); 3.81 (m, 1H); 3.74 (s, 3H); 3.03 (ddd, 1H, *J* = 1.1, 4.0, 10.8); 2.31 (ddd, 1H, *J* = 4.4, 13.9, 12.8); 2.23 (dd, 1H, *J* = 5.5, 10.8); 2.21 (s, 3H); 2.13 (dd, 1H, *J* = 4.4, 12.8); 1.78 (ddd, 1H, *J* = 5.7, 12.8, 12.8). HRMS (ESI): *m*/*z* calculated for $C_{20}H_{26}NO7^+$ [M+H$^+$] = 392.1709. Found = 392.1704.

Chemical derivations of DXM [(9α,13α,14α)-17-methyl-3-methoxymorphinan] 3

DXM 3, $C_{18}H_{25}NO$ (Generation of DXM 3 free base). A solution of NaOH (2.16 g, 5.4 mmol in 4 mL of H_2O), was added at r.t. to a suspension of dextromethorphan **3** hydrobromide monohydrate (2 g, 5.4 mmol) in 8 mL $CHCl_3$ and the resulting mixture was stirred for 30 min at r.t. The organic layer was separated, dried over $MgSO_4$ and filtered. The solvent was evaporated under reduced pressure to give **3** free base as a dense and viscous off-white oil which solidified upon standing (1.45 g, 5.3 mmol, 99 % yield). The analytical data were in accordance with the literature.[24]

2-I-DXM 11, (9α,13α,14α)-2-iodo-17-methyl-3-methoxymorphinan, $C_{18}H_{24}INO$. To a solution of DXM **3** free base (21 mg, 0.077 mmol) in MeCN (1 mL) protected from light at 0 °C was added *N*-iodosuccinimide (20 mg, 0.089 mmol) and *p*-toluenesulfonic acid monohydrate (27 mg, 0.14 mmol). The mixture was allowed to warm up to r.t. and stirred overnight. The reaction mixture was treated with water (1.5 mL) and $Na_2S_2O_3$ 1 M (1 mL)

Preprints (www.preprints.org) | NOT PEER-REVIEWED | Posted: 6 January 2022 doi:10.20944/preprints202201.0063.v1

and basified with a saturated solution of Na_2CO_3 to pH 10. The aqueous phase was extracted with CH_2Cl_2 (4 x 3 mL) and the combined organic phases were dried over Na_2SO_4 and evaporated to dryness under reduced pressure. The crude product was purified by column chromatography on silica gel using CH_2Cl_2/MeOH (100:0 to 95:5 *v*/*v* containing 1 % NEt_3) as eluent. **11** was obtained as a pale orange solid (28 mg, 0.070 mmol, 91 % yield). ^{1}H NMR ($CDCl_3$, 400 MHz): δ 7.50 (s, 1H); 6.68 (s, 1H); 3.83 (s, 3H); 2.93 (d, 1H, *J* = 18.3); 2.82-2.80 (m, 1H); 2.56 (dd, 1H, *J* = 5.7, 18.1); 2.48-2.45 (m, 1H); 2.39 (s, 3H); 2.33-2.30 (m, 1H); 2.06 (td, 1H, *J* = 3.2, 12.4); 1.87-1.83 (m, 1H); 1.77 (td, 1H, *J* = 4.8, 12.7); 1.65-1.62 (m, 2H); 1.42-1.25 (m, 5H); 1.08 (qd, 1H, *J* = 3.7, 12.5). ^{13}C NMR ($CDCl_3$, 100 MHz): δ 157.0, 142.2, 138.5, 132.2, 108.2, 83.1, 58.0, 56.6, 47.3, 45.1, 42.8, 41.8, 37.5, 36.7, 26.8, 26.5, 23.2, 22.3. HRMS (ESI): *m*/*z* calculated for $C_{18}H_{25}NOI^+$ [M+H$^+$] = 398.0975. Found = 398.0973. The analytical data were in accordance with the literature.[23]

DX 12, (9α,13α,14α)-17-methyl-3-hydroxymorphinan, $C_{17}H_{23}NO$ (*O*-Demethylation of DXM 3). A solution of dextromethorphan **3** hydrobromide monohydrate (1.61 g, 4.35 mmol) in 48 % HBr (8 mL) was heated to reflux overnight. The reaction mixture was basified to pH 8 by the addition of an aqueous NaOH 1M solution and extracted with $CHCl_3$ (5 x 20 mL). The combined organic phases were dried over $MgSO_4$ and evaporated under vacuum to furnish DX **12** as a white solid (1.02 g, 3.96 mmol, 91 % yield). An analytical sample was purified by column chromatography on silica gel using CH_2Cl_2/MeOH (98:2 to 97:3 *v*/*v* containing 1 % NEt_3) as eluent. ^{1}H NMR ($CDCl_3$, 300 MHz): δ 6.95 (d, 1H, *J* = 8.2); 6.70 (d, 1H, *J* = 2.6); 6.61 (dd, 1H, *J* = 2.6, 8.2); 2.99 (d, 1H, *J* = 18.2); 2.91-2.86 (m, 1H); 2.66 (dd, 1H, *J* = 5.8, 18.2); 2.56-2.47 (m, 1H); 2.41 (s, 3H); 2.87-2.16 (m, 2H); 1.94-1.86 (m, 1H); 1.77 (td, 1H, *J* = 4.2, 12.7); 1. 65-1.56 (m, 1H); 1.46-1.25 (m, 7H); 1.23-1.06 (m, 1H). The analytical data were in accordance with the literature.[23]

2-I-DX 13, (9α,13α,14α)-2-iodo-17-methyl-3-hydroxymorphinan, $C_{17}H_{22}INO$. To a solution of **12** (21 mg, 0.082 mmol) in MeCN (1.5 mL) protected from light at 0 °C was added *N*-iodosuccinimide (20 mg, 0.089 mmol) and *p*-toluenesulfonic acid monohydrate (27 mg, 0.14 mmol). The mixture was allowed to warm up to r.t. and stirred overnight. The reaction mixture was treated with water (1.5 mL) and $Na_2S_2O_3$ 1 M (1.5 mL) and basified with a solution of saturated Na_2CO_3 to pH 10. The aqueous phase was extracted with CH_2Cl_2 (4 x 1 mL) and the combined organic phases were dried over Na_2SO_4 and evaporated to dryness under reduced pressure. The crude product was purified by column chromatography on silica gel using CH_2Cl_2/MeOH (100:0 to 95:5 *v*/*v* containing 1 % NEt_3) as eluent to afford **13** (27 mg, 87 %).^{1}H NMR ($CDCl_3$, 400 MHz): δ 7.42 (s, 1H); 6.78 (s, 1H); 5.29 (ls, 1H); 2.95-2.91 (m, 2H); 2.66 (dd, 1H, *J* = 5.9, 18.6); 2.59-2.55 (m, 1H); 2.44 (s, 3H); 2.22-2.15 (m, 2H); 1.91-1.88 (m, 1H); 1.77 (td, 1H, *J* = 4.7, 12.9); 1.62-1.59 (m, 1H); 1.47-1.38 (m, 2H); 1.33-1.18 (m, 4H); 1.07 (qd, 1H, *J* = 3.7, 12.4). The analytical data were in accordance with the literature.[23]

(9α,13α,14α)-2,2,2-trichloroethyl-17-carboxylate-3-methoxymorphinan 14, $C_{20}H_{24}NO_3Cl_3$ (*N*-demethylation of DXM 3, *step 1*). To a solution of DXM **3** free base (1.3 g, 4.8 mmol) in toluene (3 mL), 2,2,2-trichloroethylchloroformate (800 µL, 5.8 mmol) was added. The reaction mixture was heated under reflux for 2 h then washed with 5% HCl (3 mL) followed by water (3 mL). The organic layer was separated and dried over anhydrous $MgSO_4$. Toluene was removed under reduced pressure and the crude product was purified by column chromatography on silica gel using cyclohexane/EtOAc (90:10 *v*/*v*) to afford **14** (3.1 g, 92 %) as a white solid.^{1}H NMR ($CDCl_3$, 400 MHz): Amide rotamers [7.03 and 7.00 (d, 1H, *J* = 8.4)]; 6.83 (d, 1H, *J* = 2.4); 6.73 (dd, 1H, *J* = 2.4, 8.4); 4.85 (t, 1H, *J* = 6.5); 4.75 (q, 1H, *J* = 12.0); 4. 39 (t, 1H, *J* = 4.4); 3.92 (td, 1H, *J* = 4.5, 12.8); 3.79 (s, 3H); 3.13 (dd, 1H, *J* = 6.0, 18.1); 2.79-2.26 (m, 2H); 2.38 (m, 1H); 1.74-1.26 (m, 9H); 1.09 (m, 1H). ^{13}C ($CDCl_3$, 100 MHz): δ 158.6, 153.7, 140.2, 129.1, 128.1, 111.4, 96.0, 95.1, 55.3, 50.7, 44.0, 41.7, 38.9, 37.6, 36.5, 31.4, 26.6, 26.4, 22.1. The analytical data were in accordance with the literature.[24]

***Nor*-DXM 15, (9α,13α,14α)-3-hydroxymorphinan, $C_{17}H_{23}NO$ (*N*-demethylation of DXM 3, *step 2*).** To a solution of (9α,13α,14α)-2,2,2-trichloroethyl-17-carboxylate-3-methoxy morphinan **14** (3 g, 6.93 mmol) in 90 % aqueous AcOH (30 mL) was added zinc powder (1.36 g, 20.8 mmol) in portions over 30 min. After 1 h of additional stirring the zinc

Preprints (www.preprints.org) | NOT PEER-REVIEWED | Posted: 6 January 2022 doi:10.20944/preprints202201.0063.v1

was filtered off and the solvent evaporated under reduced pressure. Toluene (6 mL) was added to solubilize the obtained dense oil, the mixture was brought to boiling then allowed to cool down in a refrigerator. The resulting white precipitate of (9α,13α,14α)-3-methoxymorphinan tetraacetozincate was filtered off and washed four times with Et_2O (5 mL). The precipitate was then dissolved in $CHCl_3$ (6 mL) and basified with a solution of NaOH 1 M. The yielded white precipitate was filtered, washed with $CHCl_3$ and the organic layer separated. The aqueous layer was further extracted with $CHCl_3$ (4x10 mL), the organic layers were combined, dried over anhydrous Na_2SO_4 and the solvent was evaporated under reduced pressure to afford *nor*-DXM **15** (0.832 g, 3.23 mmol, 47 % yield) as a clear oil which solidified upon standing. ^{1}H NMR ($CDCl_3$, 400 MHz): δ 9.55 (ls, 1H); 6.98 (d, 1H, *J* = 8.4); 6.69 (d, 1H, *J* = 2.6); 6.35 (dd, 1H, *J* = 2.6, 8.4); 3.67 (s, 3H); 3.63-3.58 (m, 1H); 3.19-3.03 (m, 3H); 2.63 (t, *J* = 12.0, 1H); 2.24 (d, 1H, *J* = 13.6); 2.08 (d, 1H, *J* = 12.0); 1.92 (td, 1H, *J* = 43.6, 13.6); 1.53 (d, 1H, *J* = 12.4); 1.46-1.25 (m, 5H); 1.21-1.12 (m, 1H); 0.96 (qd, 1H, *J* = 2.4, 12.4). The analytical data were in accordance with the literature.[24]

General procedure for the reductive animation of *nor*-DXM 15 (cpds. 16a-m). To a stirred solution of *nor*-DXM **15** (30 mg, 0.117 mmol) in anhydrous DMF (300 µL) was added the corresponding aldehyde (0.129 mmol) at r. t. under an argon atmosphere. After 10 min, STABH (97 %, 51 mg, 234 µmol) was added in one portion. The resulting suspension was stirred until completion (TLC monitoring, see table 3) then, H_2O (100 µL) was added and the reaction mixture was partitioned in a system composed of EtOAc (300 µL) and $NaHCO_3$ / Na_2CO_3 buffer (pH 9.5, 300 µL). After separation, the organic phase was washed with carbonate buffer (3 x 300 µL), dried over Na_2SO_4 and concentrated under reduced pressure. The crude product was purified by column chromatography on silica gel using cyclohexane / EtOAc (95:5 to 90:10 *v*/*v* containing 1% NEt_3) as eluent, yielding *N*-substituted (9α,13α,14α)- 3-methoxymorphinans **16a-m** in 33-97 % yield.

Table 4. Reaction times to synthesize Cpds. **16a**-**16m** by reductive amination with STABH and their yields.

Cpd.	Reaction Time (h)	Yield (%)
16a.	2	45
16b		75
16c		56
16d		56
16e		52
16f		68
16g		35
16h		68
16i		53
16j	21	48
16k	15	33
16l	2	82
16m		97

Cpd. 16a, (9α,13α,14α)-17-propyl-3-methoxymorphinan, $C_{20}H_{29}NO$. ^{1}H NMR ($CDCl_3$, 600 MHz): δ 7.02 (d, 1H, *J* = 8.3); 6.80 (d, 1H, *J* = 2.4); 6.69 (dd, 1H, *J* = 2.4, 8.3); 3.79 (s, 3H); 3.78-3.95 (m, 2H); 2.61 (dd, 1H, *J* =4.9, 17.9); 2.55 (d, 1H, *J* = 9.5); 2.51-2.45 (m, 2H); 2.34 (d, 1H, *J* = 13.3); 2.06 (t, 1H, *J* = 11); 1.86 (d, 1H, *J* = 10); 1.77 (t, 1H, *J* = 10.7); 1.63 (d, 1H, *J* = 12.1); 1.55-1.50 (m, 3H); 1.42-1.25 (m, 5H); 1.13 (qd, 1H, *J* = 3.5, 12.6); 0.93-0.90 (t, 3H, *J* = 7.2). ^{13}C NMR ($CDCl_3$, 150 MHz): δ 158.3, 141.9, 130.0, 128.6, 111.2, 110.8, 57.2, 56.1, 55.3, 46.0, 45.0, 42.0, 38.0, 36.7, 27.0, 26.7, 24.1, 22.4, 20.9, 12.2. HRMS (ESI): *m*/*z* calculated for $C_{20}H_{30}NO^+$ $[M+H]^+$ = 300.2322. Found = 300.2323.

Cpd. 16b, (9α,13α,14α)-17-butyl-3-methoxymorphinan, $C_{21}H_{31}NO$. ^{1}H NMR ($CDCl_3$, 300 MHz): δ 7.02 (d, 1H, *J* = 9.0); 6.80 (d, 1H, *J* = 3.0); 6.69 (dd, 1H, *J* = 3.0, 9.0); 3.78 (s, 3H); 2.96-2.90 (m, 2H); 2.64-2.45 (m, 4H); 2.35-2.32 (m, 1H); 2.08-2.00 (td, 1H, *J* =3.0, 9.0); 1.87-1.72 (m, 2H); 1.64-1.61 (m, 1H); 1.54-1.45 (m, 3H); 1.44-1.27 (m, 7H); 1.13-1.08 (m, 1H); 0.94-0.90 (t, 3H, *J* = 6.0). ^{13}C NMR ($CDCl_3$, 75 MHz): δ 158.2, 141.8, 129.8, 128.5, 111.1, 110.7, 55.8, 55.2, 54.8, 45.9, 45.0, 41.9, 37.9, 36.6, 29.8, 26.9, 26.6, 23.9, 22.3, 21.0, 14.2. HRMS (ESI): *m*/*z* calculated for $C_{21}H_{32}NO^+$ $[M+H]^+$ = 314.2478. Found = 314.2480.

Preprints (www.preprints.org) | NOT PEER-REVIEWED | Posted: 6 January 2022 doi:10.20944/preprints202201.0063.v1

Cpd. 16c, (9α,13α,14α)-17-pentyl-3-methoxymorphinan, $C_{22}H_{33}NO$. ^{1}H NMR ($CDCl_3$, 400 MHz): δ 7.00 (d, 1H, *J* = 8.3); 6.80 (d, 1H, *J* = 2.6); 6.69 (dd, 1H, *J* = 2.6, 8.3); 3.78 (s, 3H); 2.96-2.89 (m, 2H); 2.61 (d, 1H, *J* = 5.5); 2.56-2.44 (m, 3H); 2.33 (d, 1H, *J* = 12.3); 2.04-2.01 (m, 1H); 1.84 (d, 1H, *J* = 12.4); 1.76 (m, 1H); 1.63 (m, 1H); 1.54-1.47 (m, 3H); 1.41-1.26 (m, 9H); 1.13-1.09 (qd, 1H *J* = 2.8, 11.8); 0.89 (t, 3H, *J* = 6.8). ^{13}C NMR ($CDCl_3$, 100 MHz): δ 158.3, 142.0, 130.0, 128.6, 111.2, 110.8, 56.0, 55.3, 55.2, 46.0, 45.2, 42.0, 38.0, 36.8, 30.1, 27.5, 27.0, 26.7, 24.0, 22.8, 22.4, 14.2. HRMS (ESI): *m*/*z* calculated for $C_{22}H_{34}NO^+$ $[M+H]^+$ = 328.2635. Found = 328.2635.

Cpd. 16d, (9α,13α,14α)-17-cyclopropylmethyl-3-methoxymorphinan $C_{21}H_{29}NO$. ^{1}H NMR ($CDCl_3$, 400 MHz): δ 7.00 (d, 1H, *J* = 8.4); 6.80 (d, 1H, *J* = 2.5); 6.69 (dd, 1H, *J* = 2.5, 8.4); 3.80 (s, 3H); 3.17-3.12 (m, 1H); 2.88 (d, 1H, *J* = 18.2); 2.77-2.71 (m, 1H); 2.65-2.60 (m, 1H); 2.55-2.50 (m, 1H); 2.35 (d, 2H, *J* = 13.0); 2.03 (t, 1H, *J* = 13.2); 1.91 (d, 1H, *J* = 9.6); 1.82 (t, 1H, *J* = 11.5); 1.64 (d, 1H, *J* = 13.0); 1.55-1.49 (m, 1H); 1.44-1.27 (m, 5H); 1.15 (qd, 1H, *J* = 2.4, 12.4); 0.95-0.87 (m, 1H); 0.55-0.50 (m, 2H); 0.16-0.12 (m, 2H). ^{13}C NMR ($CDCl_3$, 100 MHz): δ 158.6, 142.1, 130.1, 128.8, 111.4, 111.1, 60.2, 56.3, 55.5, 46.2, 45.3, 42.2, 38.2, 36.9, 27.3, 26.9, 24.3, 22.6, 4.5, 4.01. HRMS (ESI): *m*/*z* calculated for $C_{21}H_{30}NO^+$ $[M+H]^+$ = 312.2322. Found = 312.2341.

Cpd. 16e, (9α,13α,14α)-17-cyclopentylmethyl-3-methoxy morphinan $C_{23}H_{33}NO$. ^{1}H NMR ($CDCl_3$, 600 MHz): δ 7.00 (d, 1H, *J* = 8.3); 6.80 (d, 1H, *J* = 2.5); 6.69 (dd, 1H, *J* = 2.2, 8.3); 3.78 (s, 3H); 2.92 (d, 1H, *J* = 17.7); 2.66-2.37 (m, 1H); 2.33 (d, 1H, *J* = 13.3); 2.13-2.00 (m, 2H); 1.86-1.71 (m, 4H); 1.66-1.56 (m, 4H); 1.54-1.50 (m, 4H); 1.42-1.20 (m, 8H); 1.10 (qd, 1H, *J* = 3.9, 12.5). HRMS (ESI): *m*/*z* calculated for $C_{21}H_{30}NO^+$ $[M+H]^+$ = 340.2635. Found = 340.2636.

Cpd. 16f, (9α,13α,14α)-17-cyclohexylmethyl-3-methoxy morphinan, $C_{24}H_{35}NO$. ^{1}H NMR ($CDCl_3$, 600 MHz): δ 7.00 (d, 1H, *J* = 8.3); 6.80 (d, 1H, *J* = 2.3); 6.68 (dd, 1H, *J* = 2.3, 8.3); 3.80 (s, 3H); 2.91 (d, 1H, *J* = 17.9); 2.79-2.75 (m, 1H); 2.58 (d, 1H, *J* = 17.0); 2.45-2.40 (m, 1H); 2.34-2.25 (m, 3H); 2.07-2.01 (m, 1H); 1.81 (d, 1H, *J* = 12.2); 1.75-1.62 (m, 6H); 1.50 (d, 1H, *J* = 11.3); 1.40-1.33 (m, 11H); 0.93-0.82 (m, 2H). ^{13}C NMR ($CDCl_3$, 150 MHz): δ 158.2, 142.2, 130.0, 128.7, 111.2, 110.7, 62.3, 56.7, 55.3, 46.3, 45.3, 42.3, 38.4, 36.8, 35.9, 32.2, 27.1, 27.0, 26.8, 26.4, 24.6, 22.4. HRMS (ESI): *m*/*z* calculated for $C_{24}H_{36}NO^+$ $[M+H]^+$ = 354.2791. Found = 354.2790.

Cpd. 16g, (9α,13α,14α)-17-(2′-furanylmethyl)-3-methoxy morphinan, $C_{22}H_{27}NO_2$. ^{1}H NMR ($CDCl_3$, 400 MHz): δ 7.39-7.38 (m, 1H); 7.04 (d, 1H, *J* = 8.4); 6.81(d, 1H, *J* = 2.6); 6.70 (dd, 1H, *J* = 2.6, 8.4); 6.31-6.30 (m, 1H); 6.24-6.20 (m, 1H); 3.79 (s, 3H); 3.70 (q, 2H, *J* = 13.8); 2.98 (d, 1H, *J* = 18.3); 2.85-2.81 (m, 1H); 2.63 (dd, 1H, *J* = 5.3, 18.2); 2.55-2.50 (m, 1H); 2.33 (d, 1H, *J* = 12.8); 2.17-2.08 (m, 1H); 1.89 (d, 1H, *J* = 12.4); 1.83-1.73 (m, 1H); 1.63-1.60 (m,1H); 1.52-1.38 (m, 1H); 1.35-1.29 (m, 5H); 1.11 (qd, 1H, *J* = 3.6, 12.4). ^{13}C NMR ($CDCl_3$, 100 MHz): δ 158.3, 142.3, 140.0, 129.8, 128.6, 111.2, 110.8, 110.2, 108.5, 55.9, 55.3, 51.9, 45.8, 44.9, 41.8, 37.9, 36.7, 27.0, 26.9, 26.7, 24.1, 22.4. HRMS (ESI): *m*/*z* calculated for $C_{22}H_{28}NO_2^+$ $[M+H]^+$ = 338.2115. Found = 338.2116.

Cpd. 16h, (9α,13α,14α)-17-(2′-thiophenylmethyl)-3-methoxymorphinan, $C_{22}H_{27}NOS$. ^{1}H NMR ($CDCl_3$, 400 MHz): δ 7.22 (d, 1H, *J* = 3.6); 7.04 (d, 1H, *J* = 8.4); 6.92 (d, 1H, *J* = 2.4); 6.81 (d, 1H, *J* = 2.4); 6.71 (dd, 1H, *J* = 2.4, 8.4); 3.94-3.78 (m, 2H); 3.79 (s, 3H); 3.01-2.91 (m, 2H); 2.64 (dd, 1H, *J* = 4.6, 17.8); 2.55 (d, 1H, *J* = 9.2); 2.34 (d, 1H, *J* = 12.8); 2.13 (t, 1H, *J* = 11.7); 1.87 (d, 1H, *J* = 11.6); 1.79-1.68 (m, 1H); 1.62 (d, 1H, *J* = 9.2); 1.52 (d, 1H, *J* = 9.2); 1.41-1.24 (m, 6H); 1.09 (qd, 1H *J* = 3.4, 12.5). ^{13}C NMR ($CDCl_3$, 100 MHz): δ 158.4, 142.1, 130.1, 128.6, 128.0, 126.5, 125.1, 124.8, 111.3, 110.8, 56.0, 55.3, 54.1, 45.6, 45.1, 42.1, 38.0, 36.7, 26.9, 26.8, 24.7, 22.4. HRMS (ESI): *m*/*z* calculated for $C_{22}H_{28}NOS^+$ $[M+H]^+$ = 354.1885. Found = 354.1885.

Cpd. 16i, (9α,13α,14α)-17-(2′-pyrrolylmethyl)-3-methoxy morphinan, $C_{22}H_{28}N_2O$. ^{1}H NMR ($CDCl_3$, 400 MHz): δ 8.75 (ls, 1H); 7.04 (d, 1H, *J* = 8.4); 6.81 (d, 1H, *J* = 2.4); 6.75 (q, 1H, *J* = 1.4); 6.70 (dd, 1H, *J* = 2.6, 8.4); 6.12 (q, 1H, *J* = 2.8); 6.03-6.00 (m, 1H); 3.79 (s, 3H); 3.70 (q, 2H, *J* = 13.8), 2.97 (d, 1H, *J* = 18.1); 2.83-2.80 (m, 1H), 2.63 (dd, 1H, *J* = 5.8, 18.2); 2.46 (dd, 1H, *J* = 3.2, 12.0); 2.38-2.33 (m, 1H); 2.13 (td, 1H, *J* = 3.0, 12.4); 1.85-1.79 (m, 1H); 1.72-1.62 (m, 2H); 1.55-1.49 (m, 1H); 1.38-1.30 (m, 5H); 1.15-1.09 (m, 1H). ^{13}C NMR ($CDCl_3$, 100 MHz): δ 158.3, 141.9, 129.9, 129.4, 128.6, 117.3, 111.3, 110.8, 108.0, 106.9, 55.8, 55.3, 52.0,

 doi:10.20944/preprints202201.0063.v1

45.6, 45.3, 42.1, 38.0, 36.8, 26.9, 26.7, 24.5, 22.4. HRMS (ESI): *m*/*z* calculated for $C_{22}H_{29}N_2O^+$ $[M+H]^+$ = 337.2274. Found = 337.2275.

Cpd. 16j, (9α,13α,14α)-17-(*N*-methyl-2′-pyrrolylmethyl)-3-methoxymorphinan, $C_{23}H_{30}N_2O$. ^{1}H NMR ($CDCl_3$, 600 MHz): δ 7.06 (d, 1H, *J* = 8.3); 6.81 (d, 1H, *J* = 1.9); 6.72 (dd, 1H *J* = 1.9, 8.3); 6.60 (s, 1H); 6.02 (s, 1H); 5.97 (s, 1H); 3.78 (s, 3H); 3.68-3.54 (m, 5H); 3.99 (d, 1H, *J* = 18.0); 2.79-2.76 (m, 1H); 2.62-2.57 (m, 1H); 2.46-2.43 (m, 1H); 2.36-2.33 (m, 1H); 2.09-2.04 (m, 1H); 1.76-1.73 (m, 1H); 1.65-1.62 (m, 2H); 1.52-1.50 (m, 1H); 1.39-1.29 (m, 5H); 1.18-1.07 (m, 1H). ^{13}C NMR ($CDCl_3$, 150 MHz): δ 158.3, 142.1, 130.3, 130.0, 128.6, 122.5, 111.3, 110.7, 109.0, 106.1, 55.4, 55.3, 53.5, 51.2, 45.5, 45.1, 42.3, 38.0, 36.8, 34.0, 26.7, 24.2, 22.4. HRMS (ESI): *m*/*z* calculated for $C_{23}H_{31}N_2O^+$ $[M+H]^+$ = 351.2431. Found = 351.2431.

Cpd. 16k, (9α,13α,14α)-17-(5′-imidazolylmethyl)-3-methoxymorphinan, $C_{22}H_{29}N_3O$. ^{1}H NMR ($CDCl_3$, 400 MHz): δ 7.44 (s, 1H); 7.00 (d, 1H, *J* = 8.4); 6.74 (d, 1H, *J* = 2.4); 6.45 (dd, 1H, *J* = 2.4, 8.4); 3.72 (s, 3H), 3.63 (q, 2H, *J* = 13.6); 2.92 (d, 1H, *J* = 18.4); 2.82-2.78 (m, 1H); 2.63 (dd, 1H, *J* = 5.2, 18.0); 2.53-2.45 (m, 1H); 2.30-2.26 (m, 1H); 2.15 (s, 3H); 1.81-1.78 (m, 1H); 1.71-1.66 (m, 1H); 1.58-1.56 (m, 1H); 1.47-1.44 (m, 1H); 1.36 (s, 3H); 1.30-1.19 (m, 4H); 1.17-0.98 (m, 1H). HRMS (ESI): *m*/*z* calculated for $C_{22}H_{30}N_3O^+$ $[M+H]^+$ = 352.2383. Found = 352.2378.

Cpd. 16l, (9α,13α,14α)-17-(2′-indolylmethyl)-3-methoxymorphinan, $C_{26}H_{30}N_2O$. ^{1}H NMR ($CDCl_3$, 400 MHz): δ 8.79 (ls, 1H); 7.54 (d, 1H, *J* = 8.0); 7.36 (d, 1H, *J* = 8.0); 7.15 (t, 1H, *J* = 7.2); 7.07 (t, 1H, *J* = 6.8); 6.81 (d, 1H, *J* = 2.0); 6.72 (dd, 1H, *J* = 2.4, 8.4); 6.33 (s, 1H); 3.88 (q, 2H, *J* = 13.6); 3.81 (s, 3H); 3.01 (d, 1H, *J* = 18.4); 2.87-2.43 (m, 1H), 2.67 (dd, 1H, *J* = 5.6, 18.0); 2.51 (dd, 1H, *J* = 3.2, 12.0); 2.33 (d, 1H, *J* = 12.8); 2.21 (td, 1H, *J* = 3.2, 12.0); 1.91-1.87 (m, 1H); 1.74 (td, 1H, *J* = 3.2, 12.4); 1.65-1.62 (m, 1H); 1.54-1.51 (m, 1H); 1.40-1.32 (m, 5H); 1.26 (t, 1H, *J* = 7.2); 1.15-1.05 (m, 1H). ^{13}C NMR ($CDCl_3$, 100 MHz): δ 158.3, 136.1, 128.6, 128.5, 121.5, 120.1, 119.6, 111.2, 110.8, 56.0, 55.2, 52.3, 45.7, 41.8, 37.8, 36.6, 26.7, 26.5, 24.6, 22.2. HRMS (ESI): *m*/*z* calculated for $C_{26}H_{31}N_2O^+$ $[M+H]^+$ = 387.2436. Found = 387.2425.

Cpd. 16m, (9α,13α,14α)-17-(2′-(2′′,2′′′-bithiophenyl) methyl)-3-methoxymorphinan, $C_{26}H_{29}NOS_2$. ^{1}H NMR ($CDCl_3$, 400 MHz): δ 7.18 (d, 1H, *J* = 5.2); 7.14 (d, 1H, *J* = 3.2); 7.06 (d, 1H, *J* = 8.4); 7.01-6.98 (m, 2H); 6.82 (d, 1H, *J* = 2.0); 6.72 (dd, 1H, *J* = 2.4, 8.4); 3.92-3.81 (m, 2H); 3.82 (s, 3H); 2.99-2.95 (m, 2H); 2.71-2.66 (m, 2H); 2.35 (d, 1H, *J* = 12.8); 2.07-2.03 (m, 1H); 1.92-1.89 (m, 1H); 1.82-1.78 (m, 1H); 1.64-1.62 (m, 1H); 1.54 (d, 1H, *J* = 11.6); 1.41-1.24 (m, 6H); 1.10 (qd, 1H, *J* = 4.0, 12.4). HRMS (ESI): *m*/*z* calculated for $C_{26}H_{30}NOS_2^+$ $[M+H]^+$ = 436.1769. Found = 436.1757.

Cpd. 17, (9α,13α,14α)-17-cyclopropylmethyloxy-3-methoxymorphinan, $C_{21}H_{27}NO_2$. A solution of *nor*-DXM **15** (36 mg, 0.140 mmol) in CH_2Cl_2 (500 µL) was cooled to 0°C then NEt_3 (20 µL) and cyclopropanecarbonyl chloride (16 mg, 0.153 mmol). The reaction mixture was stirred from 0°C to room temperature for 1.5h. The reaction mixture was washed with $NaHCO_3$ / Na_2CO_3 buffer (pH 9.5, 500 µL). The organic layer was dried over $MgSO_4$, filtered and concentrated under reduced pressure. The crude product was purified by column chromatography using silica gel and cyclohexane / EtOAc (100:0 to 80:20 *v*/*v* containing 1 % NEt_3) as eluent to afford **17** (34 mg, 75 %).^{1}H NMR ($CDCl_3$, 400 MHz): δ 7.02 (d, 1H, *J* = 8.4); 6.84 (d, 1H, *J* = 2.6); 6.72 (dd, 1H, *J* = 2.6, 8.4); 4.76-4.65 (m, 1H); 4.09-4.03 (m, 1H,); 3.79 (s, 3H); 3.13 (dd, 1H, *J* = 6.0, 18.0); 2.66 (d, 1H, *J* = 17.6); 2.40-2.36 (m, 1H); 1.74-1.24 (m, 11H); 1.14-1.04 (m, 1H); 0.98-0.94 (m, 1H); 0.76-0.71 (m, 1H). ^{13}C NMR ($CDCl_3$, 100 MHz): δ 171.9, 158.6, 140.6, 129.2, 128.5, 111.5, 111.3, 55.4, 44.2, 42.1, 38.0, 36.6, 31.6, 26.7, 22.2, 11.6, 7.4, 7.2. HRMS (ESI): *m*/*z* calculated for $C_{21}H_{27}NO_2Na^+$ $[M+Na]^+$ = 348.1934. Found = 348.1935.

Cpd. 18, (9α,13α,14α)-17,17-dimethyl-3-methoxy morphinan iodide, $C_{19}H_{28}NOI$. To a solution of DXM **3** free base (30 mg 0.11 mmol) in CH_2Cl_2 (300 µL) was added CH_3I (300 µL, 4.82 mmol) and the mixture was stirred for 2 h at r.t. The obtained white precipitate was filtered and washed with EtOAc (4 x 300 µL) to give **18** as a white powder (26 mg, 0.091 mmol, 82 % yield). ^{1}H NMR ($CDCl_3$, 400 MHz): δ 7.12 (d, 1H, *J* = 9.2); 6.80-6.77 (m, 2H); 4.10-4.07 (m, 1H); 3.58 (s, 3H); 3.69 (s, 3H); 3.61-3.55 (m, 1H); 3.52 (s, 3H); 3.38-3.32 (m, 1H); 2.87-2.85 (m, 1H); 2.43-2.36 (m, 2H); 2.14-2.12 (m, 1 H); 1.74-1.44 (m, 6H); 1.33-1.22 (m, 1H); 1.12 (qd, 1H, *J* = 3.6, 12.4). ^{13}C NMR ($CDCl_3$, 100 MHz): δ 159.7, 138.6, 129.5, 124.1,

Preprints (www.preprints.org) | NOT PEER-REVIEWED | Posted: 6 January 2022 doi:10.20944/preprints202201.0063.v1

112.6, 111.4, 69.6, 57.7, 55.5, 54.5, 51.2, 38.7, 36.8, 36.5, 35.5, 26.7, 26.4, 25.9, 21.8. HRMS (ESI): *m/z* calculated for $C_{19}H_{28}NO^+$ [M^+] = 286.2171. Found = 286.2166.

Drug preparation and storage. Tazopsine **1**, DXM **3** and derivatives (cpds. **6**-**18**) were prepared in DMSO at 10 mM, aliquoted then stored at -20 °C. PQ and CQ biphosphates were prepared at 110 mM and 132 µM, respectively in sterile water, aliquoted then stored at -20 °C. A stock aliquot was thawed and used for daily medium changes of the parasite cultures whenever necessary.

Parasite maintenance and inhibition assays (by order of appearance in the manuscript).

P. yoelii growth inhibition assays in vitro.

Parasite culture. *P. yoelii* (265 BY strain) sporozoites were obtained by dissection of infected *Anopheles stephensi* salivary glands. Primary mouse hepatocytes were isolated as previously described[31] and seeded in eight-well Lab-Tek plastic chamber slides (VWR, Fontenay-sous-Bois, France) previously coated with rat-tail collagen I (BD Biosciences, Le Pont de Claix, France) at a density of 105 cells per well. Mouse hepatocytes were cultured at 37 °C in 5 % CO_2 in William's E medium supplemented with 10 % fetal calf serum, 1 % L-glutamine, 1 % sodium pyruvate, 1 % insulin-transferrin-selenium, 1 % nonessential amino acids, and 1 % penicillin-streptomycin (all from Invitrogen, Cergy-Pontoise, France), for 24 h before inoculation of *P. yoelii* sporozoites (105 per well). Test cpds. were solubilized in DMSO, further diluted in culture medium (equal DMSO concentrations of < 0.3 % per well), and then added to hepatocyte cultures at the time of sporozoite inoculation. 3 h later, after sporozoite penetration into hepatocytes, cultures were washed and further incubated in the presence of each test cpd. Culture medium containing the appropriate cpd. concentration was changed daily until 48 h.

IC_{50} measurement. Parasites were quantified on the last day of incubation by immunofluorescence analysis following fixation of the cultures with cold methanol and parasite-specific staining by a mouse polyclonal serum raised against the *P. yoelii* heat shock protein 70 and revealed with FITC-conjugated goat anti-mouse immunoglobulin (Sigma). Parasite numbers were counted under a fluorescence microscope with a 25× light microscope objective. IC_{50} values, the compound concentration at which a 50 % reduction in the number of parasites was observed, as compared to the number in the DMSO control cultures, were calculated by linear regression using Excel software and derived from three independent experiments, where each concentration was tested in triplicates.

P. berghei growth inhibition assays in vivo.

This study was performed according to Bosson Vanga *et al.*[32] Six to eight week-old BALB/c female mice were obtained from Janvier CERJ (Le Genest-Saint-Isle, France) and housed in CEF (UMS28, La Pitié-Salpêrière) under pathogen-free conditions with food and water *ad libitum*. All animal work was conducted in strict accordance with the Directive 2010/63/EU of the European Parliament and Council "On the protection of animals used for scientific purposes". Protocols were approved by the Ethical Committee Charles Darwin N°005 (approval #01736.02). Five mice were used per treatment group. Drugs were administrated on days − 1, 0, +1, and mice were challenged on day 0 by retro-orbital injection of *P. berghei* (GFP-luc strain) sporozoites (10,000 per mouse). *In vivo* imaging was performed 44 h post-infection to assess liver stage development. IVIS Spectrum (Caliper Life Science, Hanover, MD, USA) was used to measure luminescence expressed as total flux photon/seconde. Prior to analysis, mice were injected *ip* with D-luciferin (100 mg/kg), anesthetized with isoflurane and imaged 10 min post-injection. Images were analysed using the living Image 3.0 software (Capiler Life Science, Hanover, MD, USA). Data analysis and statistical analysis using a one-way ANOVA test for multiple comparisons were done with GraphPad Prism 8 statistical Software (GraphPad. Software, San Diego, CA, USA).

P. falciparum and P. berghei liver stages growth inhibition assays in vitro.

Parasite culture. *Plasmodium* liver stages were cultured as described elsewhere (Baron *et al.* manuscript in preparation). Briefly, cryopreserved primary human

Preprints (www.preprints.org) | NOT PEER-REVIEWED | Posted: 6 January 2022 doi:10.20944/preprints202201.0063.v1

hepatocytes were purchased from Lonza Bioscience and Biopredic International (Saint-Grégoire, France). Cells were thawed and seeded in 384-well plates (Greiner Bio-One, Germany) pre-coated with rat-tail collagen I (BD Bioscience, USA). Human hepatocytes were maintained at 37°C in 5 % CO2 in William's E medium (Gibco) supplemented with 10 % fetal clone III serum (FCS, Hyclone), 100 u/mL penicillin and 100 ug/mL streptomycin (Gibco), 5 × 10−3 g/L human insulin (Sigma-Merck), 5 × 10−5 M hydrocortisone (Upjohn Laboratories SERB, France). The next day, cells were overlaid with matrigel (Corning) and medium was then renewed every two days. Four days later, sporozoite were isolated by aseptic hand dissection of salivary glands of *P. berghei*-GFP[33] or *P. falciparum*-infected mosquitoes (*P. falciparum* NF54 strain, obtained from Department of Medical Microbiology, University Medical Centre, St Radboud, Nijmegen, The Netherlands). Matrigel was then removed from hepatocyte culture and 5,000 or 30,000 sporozoites of *P. berghei*-GFP or, *P. falciparum* were inoculated to cells before centrifugation at 560 xg for 10 min at RT and incubation at 37°C, 5 % CO2. Drugs were tested in quadruplicate, starting from time of sporozoite addition. 3 h later, infected cultures were covered with matrigel prior to addition of fresh cell culture medium containing the appropriate drug dilutions. Medium, containing drug or not, was renewed on a daily basis, until cell fixation, 48 h and 6 days post-infection with *P. berghei* and *P. falciparum* sporozoites respectively.

Immunostaining of P. berghei and P. falciparum liver stages.

Infected cultures were fixed using 4% paraformaldehyde (PFA) for 15 min at r.t. and liver stage parasites were immune-labeled with polyclonal anti-PfHSP70 murine serum revealed with Alexa-Fluor 488-conjugated goat anti-mouse immunoglobulin (Invitrogen). DAPI was used to visualize nuclei.

Parasite enumeration and toxicity assessment using high-content imaging. Upon fixation and immunostaining, cell culture plates were analyzed in order to determine the number and size of the parasites using a CellInsight High Content Screening platform equipped with the Studio HCS software (Thermo Fisher Scientific). Parasite size reduction was calculated on the average object area using the total surface area of each selected object (µm²) using the high content imaging approach described previously.[28] Analysis of compound cytotoxicity was performed by counting host cell nuclei on the DAPI channel.

IC_{50} measurement. C_{50} values were determined by non-linear regression with GraphPad Prism 8 software. The logarithm of concentrations was expressed in function of the parasites number normalized to the drug free controls. The tests on 384-well plates were done in quadruplicates.

Statistical Analysis. GraphPad Prism 8 (GraphPad. Software, San Diego, CA, USA) and Excel 2016 (Microsoft Office) were used in this study for the data analysis. All graph values represent means and error bar standard deviations (s. d.).

P. falciparum asexual blood stages.

Parasite culture. Chloroquine-sensitive (3D7) *P. falciparum* strain was obtained from the Malaria Research and Reference Reagent Resource Center (MR4). Parasites were maintained in human erythrocytes (O^+, provided by Etablissement français du sang, EFS, France) at 5 % haematocrit, suspended in complete culture medium RPMI 1640 medium supplemented with 25 mM HEPES, 20 mM D-glucose, 25 mM sodium bicarbonate, 0.4 mM hypoxanthine, 5 mM L-Glutamine and 10 % AB human serum. Parasite cultures were kept at 37 °C in a gaseous environment composed of 5 % CO_2, 10 % O_2 and 85 % N_2. The culture medium was changed daily, with control of parasitaemia using light microscopy (Axioskop microscope, ZEISS, Germany) under oil immersion, after fixing thin blood smears with methanol and staining with Diff-Quik™ stain Set (RAL Diagnostics, France).

IC_{50} measurement. 50% inhibitory concentrations (IC_{50}) determination test was carried out by isotopic 42 h ^{3}H-hypoxanthine incorporation assays as previously described[34] with minor modifications. Briefly, *P. falciparum* cultures at ring-stage were highly synchronized by two consecutive treatments with 5 % sorbitol (Merck-Sigma) in PBS (v/v) at 40 h intervals and diluted down to 0.3-0.5 % parasitaemia and 2 % haematocrit. Parasites

 doi:10.20944/preprints202201.0063.v1

were dispensed into 96-well plates containing 14 serially diluted concentrations of drug ranging from 0 to 240 μM, and incubated as described above in presence of 5 % ^{3}H-hypoxanthine (Perkin Elmer, USA) for 42 h. ^{3}H-hypoxanthine uptake was then evaluated by scintillation counting (Top Count NXT, Perkin Elmer, USA) and results were expressed as the inhibitory concentrations IC_{50} defined as drug concentrations at which 50 % of ^{3}H-hypoxanthine incorporation was inhibited compared with drug-free controls. IC_{50} values were established by non-linear regression with ICEstimator software (http://www.antimalarial-icestimator.net/).[35-36] The tests on 96-well plates were done in triplicates.

P. falciparum sexual blood stages.

Parasite culture and gametocyte production. The *P. falciparum* transgenic line NF54-cg6-Pfs16-CBG99 has been described elsewhere.[37-38] Parasites were cultivated *in vitro* under standard conditions using RPMI 1640 medium supplemented with 10 % heat-inactivated human serum and human erythrocytes at a 5 % hematocrit. To obtain synchronous asexual stages, parasites were synchronized by the isolation of schizonts by magnetic isolation using a MACS depletion column (Miltenyi Biotec) in conjunction with a magnetic separator, then placed back into culture. After invasion of merozoites, a second magnetic isolation was used for the selection of ring-stage parasites to obtain a tighter window of synchronization. Synchronous production of specific gametocytes stages was achieved by treating synchronized cultures at the ring stage (10–15 % parasitemia, day 0) with 50 mM *N*-acetylglucosamine (NAG) for 5 days to eliminate asexual parasites. Gametocyte preparations were enriched in different experiments by magnetic isolation.

IC_{50} measurement. To calculate the IC_{50} for DXM **3** and *N*-2'-pyrrolylmethyl-*nor*-DXM **16i** on early and mature gametocytes, 2×10^{5} MACS-purified early GIE (day 2 post NAG treatment) and mature GIE (days 7 post NAG treatment) from the NF54-cg6-Pfs16-CBG99 line were incubated with serial dilutions of inhibitors or 2 % DMSO for 72 h. After 72h, GIE were washed and cell viability was evaluated by adding a non-lysing formulation of 0.5 mM D-luciferin substrate[33] and by measuring luciferase activity for 1 s on a plate Reader Infinite 200 PRO (Tecan®). The tests on 96-well plates were performed in triplicates.

Author Contributions: The manuscript was written through contributions of all authors. All authors have given approval to the final version of the manuscript. ‡These authors contributed equally.

Funding: We thank the Doctoral School of Paris University (ED 563, MTCI) for financial support (PhD fellowship to AK).

Acknowledgments: We thank Jocelyne Roman for helping with the evaluation of the prophylactic activity of DXM **3** in mice infected with *P. berghei*, Mr Thierry Houpert for his invaluable help for the breeding of Anopheles mosquitoes, and Dr Jérôme Clain for relevant suggestions regarding the manuscript. This work benefited from equipment and services from the CELIS cell culture core facility (Institut du Cerveau et de la Moëlle Epinière, Paris), a platform supported through ANR grants number ANR-10-IAIHU-06 and ANR-11-INBS-0011- NeurATRIS. IDMIT infrastructure is supported by the French government Program d'Investissements d'Avenir (PIA) under grant number ANR-11-INBS-0008 (INBS IDMIT). This work was partly supported by the OrganoMal Project funded by the French National Agency for Research (ANR) (ANR – CE17- 0035-0011) and the PAR-AFRAP LabEx of the French Parasitology Alliance For Health Care (ANR-11-LABX-0024). LVA was supported by a CIFRE ANRT allocation N°181029A20. We are particularly grateful to David Akbar for his valuable assistance regarding automated fluorescence imaging.

Conflicts of Interest: The authors have no conflict of interest to declare.

Abbreviations: Ac_2O: Acetic anhydride; AcOH, Acetic acid; ACT, Artemisinin Combination Therapies; ARTDs, Artemisin derivatives; Bu, Butane; cpd., compound; CNS, Central nervous system; CQ, Chloroquine; DAPI, 4',6-diamidino-2-phenylindole; DMF, *N*,*N*-Dimethylformamide; DX, Dextrorphan; DXM, Dextromethorphan; EEFs, Exo-Erythrocytic Forms; Et_3N, Triethyl amine; Et_2O, Diethyl ether; EtOAc, Ethyl Acetate; GFP, Green Florescent Protein; HRMS, High-resolution mass spectra; IC_{50}, Half-maximal inhibitory concentration; IE, infected erythrocytes; Me, methyl; MeCN, Acetonitrile; MeI, Methyl iodide; MeOH, methanol, NIS, *N*-iodosuccinimide; NMDA, *N*-methyl-D-

aspartate; NMR, Nuclear Magnetic Resonance; *Pb*, *Plasmodium berghei*; Pent, Pentane; *Pf*, *Plasmodium falciparum*; *Py*, *P. yoelii*; PHH, primary human hepatocyte, PMH, primary mice hepatocytes; PQ, Primaquine; Pro, Propane; QND, Quinidine; rpm, rotation per minute; r.t., room temperature; SGs, Salivary Glands; STABH, sodium triacetoxyborohydride; TLC, thin layer chromatography.

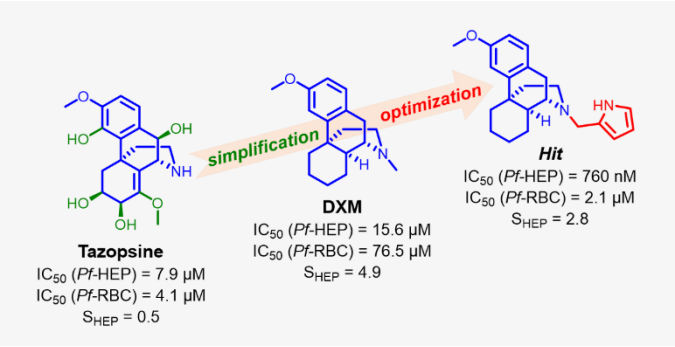

Validation of the common drug dextromethorphan as a simplified mimic of the antiplasmodial alkaloid tazopsine led to a novel potent hit compound in the *ent*-morphinane series.

References

1. WHO, World Malaria report. **2019**.
2. Ritchie, H.; Roser, M., Causes of Death. *Our World in Data* **2018**.
3. Bhatt, S.; Weiss, D. J.; Cameron, E.; Bisanzio, D.; Mappin, B.; Dalrymple, U.; Battle, K. E.; Moyes, C. L.; Henry, A.; Eckhoff, P. A.; Wenger, E. A.; Briet, O.; Penny, M. A.; Smith, T. A.; Bennett, A.; Yukich, J.; Eisele, T. P.; Griffin, J. T.; Fergus, C. A.; Lynch, M.; Lindgren, F.; Cohen, J. M.; Murray, C. L. J.; Smith, D. L.; Hay, S. I.; Cibulskis, R. E.; Gething, P. W., The effect of malaria control on Plasmodium falciparum in Africa between 2000 and 2015. *Nature* **2015,** *526* (7572), 207-211.
4. Phillips, M. A.; Burrows, J. N.; Manyando, C.; van Huijsduijnen, R. H.; Van Voorhis, W. C.; Wells, T. N. C., Malaria. *Nat Rev Dis Primers* **2017,** *3*, 17050.
5. Imwong, M.; Suwannasin, K.; Kunasol, C.; Sutawong, K.; Mayxay, M.; Rekol, H.; Smithuis, F. M.; Hlaing, T. M.; Tun, K. M.; van der Pluijm, R. W.; Tripura, R.; Miotto, O.; Menard, D.; Dhorda, M.; Day, N. P. J.; White, N. J.; Dondorp, A. M., The spread of artemisinin-resistant Plasmodium falciparum in the Greater Mekong subregion: a molecular epidemiology observational study. *Lancet Infect Dis* **2017,** *17* (5), 491-497.
6. Ikeda, M.; Kaneko, M.; Tachibana, S. I.; Balikagala, B.; Sakurai-Yatsushiro, M.; Yatsushiro, S.; Takahashi, N.; Yamauchi, M.; Sekihara, M.; Hashimoto, M.; Katuro, O. T.; Olia, A.; Obwoya, P. S.; Auma, M. A.; Anywar, D. A.; Odongo-Aginya, E. I.; Okello-Onen, J.; Hirai, M.; Ohashi, J.; Palacpac, N. M. Q.; Kataoka, M.; Tsuboi, T.; Kimura, E.; Horii, T.; Mita, T., Artemisinin-Resistant Plasmodium falciparum with High Survival Rates, Uganda, 2014-2016. *Emerg Infect Dis* **2018,** *24* (4), 718-726.
7. Uwimana, A.; Umulisa, N.; Venkatesan, M.; Svigel, S. S.; Zhou, Z.; Munyaneza, T.; Habimana, R. M.; Rucogoza, A.; Moriarty, L. F.; Sandford, R.; Piercefield, E.; Goldman, I.; Ezema, B.; Talundzic, E.; Pacheco, M. A.; Escalante, A. A.; Ngamije, D.; Mangala, J. N.; Kabera, M.; Munguti, K.; Murindahabi, M.; Brieger, W.; Musanabaganwa, C.; Mutesa, L.; Udhayakumar, V.; Mbituyumuremyi, A.; Halsey, E. S.; Lucchi, N. W., Association of Plasmodium falciparum kelch13 R561H genotypes with delayed parasite clearance in Rwanda: an open-label, single-arm, multicentre, therapeutic efficacy study. *Lancet Infect Dis* **2021,** *21* (8), 1120-1128.
8. Balikagala, B.; Fukuda, N.; Ikeda, M.; Katuro, O. T.; Tachibana, S. I.; Yamauchi, M.; Opio, W.; Emoto, S.; Anywar, D. A.; Kimura, E.; Palacpac, N. M. Q.; Odongo-Aginya, E. I.; Ogwang, M.; Horii, T.; Mita, T., Evidence of Artemisinin-Resistant Malaria in Africa. *N Engl J Med* **2021,** *385* (13), 1163-1171.
9. Witkowski, B.; Amaratunga, C.; Khim, N.; Sreng, S.; Chim, P.; Kim, S.; Lim, P.; Mao, S.; Sopha, C.; Sam, B.; Anderson, J. M.; Duong, S.; Chuor, C. M.; Taylor, W. R.; Suon, S.; Mercereau-Puijalon, O.; Fairhurst, R. M.; Menard, D., Novel phenotypic assays for the detection of artemisinin-resistant Plasmodium falciparum malaria in Cambodia: in-vitro and ex-vivo drug-response studies. *Lancet Infect Dis* **2013,** *13* (12), 1043-9.
10. Bloland, P. B.; Ettling, M., Making malaria-treatment policy in the face of drug resistance. *Ann Trop Med Parasitol* **1999,** *93* (1), 5-23.
11. Derbyshire, E. R.; Prudencio, M.; Mota, M. M.; Clardy, J., Liver-stage malaria parasites vulnerable to diverse chemical scaffolds. *Proc Natl Acad Sci U S A* **2012,** *109* (22), 8511-6.
12. Kato, N.; Comer, E.; Sakata-Kato, T.; Sharma, A.; Sharma, M.; Maetani, M.; Bastien, J.; Brancucci, N. M.; Bittker, J. A.; Corey, V.; Clarke, D.; Derbyshire, E. R.; Dornan, G. L.; Duffy, S.; Eckley, S.; Itoe, M. A.; Koolen, K. M.; Lewis, T. A.; Lui, P. S.; Lukens, A. K.; Lund, E.; March, S.; Meibalan, E.; Meier, B. C.; McPhail, J. A.; Mitasev, B.; Moss, E. L.; Sayes, M.; Van Gessel, Y.; Wawer, M. J.; Yoshinaga, T.; Zeeman, A. M.; Avery, V. M.; Bhatia, S. N.; Burke, J. E.; Catteruccia, F.; Clardy, J. C.; Clemons, P. A.; Dechering, K. J.; Duvall, J. R.; Foley, M. A.; Gusovsky, F.; Kocken, C. H.; Marti, M.; Morningstar, M. L.; Munoz, B.; Neafsey, D. E.; Sharma, A.; Winzeler, E. A.; Wirth, D. F.; Scherer, C. A.; Schreiber, S. L., Diversity-oriented synthesis yields novel multistage antimalarial inhibitors. *Nature* **2016,** *538* (7625), 344-349.
13. Le Manach, C.; Dam, J.; Woodland, J. G.; Kaur, G.; Khonde, L. P.; Brunschwig, C.; Njoroge, M.; Wicht, K. J.; Horatscheck, A.; Paquet, T.; Boyle, G. A.; Gibhard, L.; Taylor, D.; Lawrence, N.; Yeo, T.; Mok, S.; Eastman, R. T.; Dorjsuren, D.; Talley, D. C.; Guo, H.; Simeonov, A.; Reader, J.; van der Watt, M.; Erlank, E.; Venter, N.; Zawada, J. W.; Aswat, A.; Nardini, L.; Coetzer, T. L.; Lauterbach, S. B.; Bezuidenhout, B. C.; Theron, A.; Mancama, D.; Koekemoer, L. L.; Birkholtz, L. M.; Wittlin, S.; Delves, M.; Ottilie, S.; Winzeler, E. A.; von Geldern, T. W.; Smith, D.; Fidock, D. A.; Street, L. J.; Basarab, G. S.; Duffy, J.; Chibale, K., Identification and Profiling of a Novel Diazaspiro[3.4]octane Chemical Series Active against Multiple Stages of the Human Malaria Parasite Plasmodium falciparum and Optimization Efforts. *J Med Chem* **2021**.
14. Carraz, M.; Jossang, A.; Franetich, J. F.; Siau, A.; Ciceron, L.; Hannoun, L.; Sauerwein, R.; Frappier, F.; Rasoanaivo, P.; Snounou, G.; Mazier, D., A plant-derived morphinan as a novel lead compound active against malaria liver stages. *PLoS Med* **2006,** *3* (12), e513.

15. Carraz, M.; Jossang, A.; Rasoanaivo, P.; Mazier, D.; Frappier, F., Isolation and antimalarial activity of new morphinan alkaloids on Plasmodium yoelii liver stage. *Bioorg Med Chem* **2008,** *16* (11), 6186-92.
16. Zahari, A.; Cheah, F. K.; Mohamad, J.; Sulaiman, S. N.; Litaudon, M.; Leong, K. H.; Awang, K., Antiplasmodial and antioxidant isoquinoline alkaloids from Dehaasia longipedicellata. *Planta Med* **2014,** *80* (7), 599-603.
17. Oh, S. R.; Agrawal, S.; Sabir, S.; Taylor, A., Dextromethorphan. In *StatPearls*, Treasure Island (FL), 2021.
18. Shin, E. J.; Bach, J. H.; Lee, S. Y.; Kim, J. M.; Lee, J.; Hong, J. S.; Nabeshima, T.; Kim, H. C., Neuropsychotoxic and neuroprotective potentials of dextromethorphan and its analogs. *J Pharmacol Sci* **2011,** *116* (2), 137-48.
19. Annoura, T.; Chevalley, S.; Janse, C. J.; Franke-Fayard, B.; Khan, S. M., Quantitative analysis of Plasmodium berghei liver stages by bioluminescence imaging. *Methods Mol Biol* **2013,** *923*, 429-43.
20. Schadel, M.; Wu, D.; Otton, S. V.; Kalow, W.; Sellers, E. M., Pharmacokinetics of dextromethorphan and metabolites in humans: influence of the CYP2D6 phenotype and quinidine inhibition. *J Clin Psychopharmacol* **1995,** *15* (4), 263-9.
21. Capon, D. A.; Bochner, F.; Kerry, N.; Mikus, G.; Danz, C.; Somogyi, A. A., The influence of CYP2D6 polymorphism and quinidine on the disposition and antitussive effect of dextromethorphan in humans. *Clin Pharmacol Ther* **1996,** *60* (3), 295-307.
22. Gorski, J. C.; Jones, D. R.; Wrighton, S. A.; Hall, S. D., Characterization of dextromethorphan N-demethylation by human liver microsomes. Contribution of the cytochrome P450 3A (CYP3A) subfamily. *Biochem Pharmacol* **1994,** *48* (1), 173-82.
23. Jakobsson, J. E.; Riss, P. J., Transition metal free, late-stage, regiospecific, aromatic fluorination on a preparative scale using a KF/crypt-222 complex. *RSC Adv.* **2018,** *8* (38), 21288-21291.
24. Jozwiak, K.; Targowska-Duda, K. M.; Kaczor, A. A.; Kozak, J.; Ligeza, A.; Szacon, E.; Wrobel, T. M.; Budzynska, B.; Biala, G.; Fornal, E.; Poso, A.; Wainer, I. W.; Matosiuk, D., Synthesis, in vitro and in vivo studies, and molecular modeling of N-alkylated dextromethorphan derivatives as non-competitive inhibitors of alpha3beta4 nicotinic acetylcholine receptor. *Bioorg Med Chem* **2014,** *22* (24), 6846-56.
25. Abdel-Magid, A. F.; Carson, K. G.; Harris, B. D.; Maryanoff, C. A.; Shah, R. D., Reductive Amination of Aldehydes and Ketones with Sodium Triacetoxyborohydride. Studies on Direct and Indirect Reductive Amination Procedures(1). *J Org Chem* **1996,** *61* (11), 3849-3862.
26. Adjalley, S. H.; Johnston, G. L.; Li, T.; Eastman, R. T.; Ekland, E. H.; Eappen, A. G.; Richman, A.; Sim, B. K.; Lee, M. C.; Hoffman, S. L.; Fidock, D. A., Quantitative assessment of Plasmodium falciparum sexual development reveals potent transmission-blocking activity by methylene blue. *Proc Natl Acad Sci U S A* **2011,** *108* (47), E1214-23.
27. Cabrera, M.; Cui, L., In Vitro Activities of Primaquine-Schizonticide Combinations on Asexual Blood Stages and Gametocytes of Plasmodium falciparum. *Antimicrob Agents Chemother* **2015,** *59* (12), 7650-6.
28. Bergmann, C.; van Loon, W.; Habarugira, F.; Tacoli, C.; Jager, J. C.; Savelsberg, D.; Nshimiyimana, F.; Rwamugema, E.; Mbarushimana, D.; Ndoli, J.; Sendegeya, A.; Bayingana, C.; Mockenhaupt, F. P., Increase in Kelch 13 Polymorphisms in Plasmodium falciparum, Southern Rwanda. *Emerg Infect Dis* **2021,** *27* (1), 294-296.
29. Uwimana, A.; Legrand, E.; Stokes, B. H.; Ndikumana, J. M.; Warsame, M.; Umulisa, N.; Ngamije, D.; Munyaneza, T.; Mazarati, J. B.; Munguti, K.; Campagne, P.; Criscuolo, A.; Ariey, F.; Murindahabi, M.; Ringwald, P.; Fidock, D. A.; Mbituyumuremyi, A.; Menard, D., Emergence and clonal expansion of in vitro artemisinin-resistant Plasmodium falciparum kelch13 R561H mutant parasites in Rwanda. *Nat Med* **2020,** *26* (10), 1602-1608.
30. Borch, R. F.; Bernstein, M. D.; Dupont Durst, H., Cyanohydridoborate anion as a selective reducing agent. *J. Am. Chem. Soc.* **1971,** *93* (12), 2897-2904.
31. Renia, L.; Mattei, D.; Goma, J.; Pied, S.; Dubois, P.; Miltgen, F.; Nussler, A.; Matile, H.; Menegaux, F.; Gentilini, M.; Mazier, D., A Malaria Heat-Shock-Like Determinant Expressed on the Infected Hepatocyte Surface Is the Target of Antibody-Dependent Cell-Mediated Cytotoxic Mechanisms by Nonparenchymal Liver-Cells. *Eur J Immunol* **1990,** *20* (7), 1445-1449.
32. Bosson-Vanga, H.; Franetich, J. F.; Soulard, V.; Sossau, D.; Tefit, M.; Kane, B.; Vaillant, J. C.; Borrmann, S.; Muller, O.; Dereuddre-Bosquet, N.; Le Grand, R.; Silvie, O.; Mazier, D., Differential activity of methylene blue against erythrocytic and hepatic stages of Plasmodium. *Malar J* **2018,** *17* (1), 143.
33. Manzoni, G.; Briquet, S.; Risco-Castillo, V.; Gaultier, C.; Topcu, S.; Ivanescu, M. L.; Franetich, J. F.; Hoareau-Coudert, B.; Mazier, D.; Silvie, O., A rapid and robust selection procedure for generating drug-selectable marker-free recombinant malaria parasites. *Sci Rep* **2014,** *4*, 4760.
34. Desjardins, R. E.; Canfield, C. J.; Haynes, J. D.; Chulay, J. D., Quantitative assessment of antimalarial activity in vitro by a semiautomated microdilution technique. *Antimicrob Agents Chemother* **1979,** *16* (6), 710-8.
35. Le Nagard, H.; Vincent, C.; Mentre, F.; Le Bras, J., Online analysis of in vitro resistance to antimalarial drugs through nonlinear regression. *Comput Methods Programs Biomed* **2011,** *104* (1), 10-8.
36. Kaddouri, H.; Nakache, S.; Houze, S.; Mentre, F.; Le Bras, J., Assessment of the drug susceptibility of Plasmodium falciparum clinical isolates from africa by using a Plasmodium lactate dehydrogenase immunodetection assay and an inhibitory maximum effect model for precise measurement of the 50-percent inhibitory concentration. *Antimicrob Agents Chemother* **2006,** *50* (10), 3343-9.
37. Bouyer, G.; Barbieri, D.; Dupuy, F.; Marteau, A.; Sissoko, A.; N'Dri, M. E.; Neveu, G.; Bedault, L.; Khodabux, N.; Roman, D.; Houze, S.; Siciliano, G.; Alano, P.; Martins, R. M.; Lopez-Rubio, J. J.; Clain, J.; Duval, R.; Egee, S.; Lavazec, C., Plasmodium falciparum sexual parasites regulate infected erythrocyte permeability. *Commun Biol* **2020,** *3* (1), 726.
38. Cevenini, L.; Camarda, G.; Michelini, E.; Siciliano, G.; Calabretta, M. M.; Bona, R.; Kumar, T. R.; Cara, A.; Branchini, B. R.; Fidock, D. A.; Roda, A.; Alano, P., Multicolor bioluminescence boosts malaria research: quantitative dual-color assay and single-cell imaging in Plasmodium falciparum parasites. *Anal Chem* **2014,** *86* (17), 8814-21.